# NAVAL POSTGRADUATE SCHOOL
## Monterey, California

AD-A276 742

DTIC
ELECTE
MAR 14 1994
S
F
D

# THESIS

**GRAPHICAL MODELING OF SHIPBOARD ELECTRIC POWER DISTRIBUTION SYSTEMS**

by

Daniel B. Kline

December 1993

Thesis Advisor:                                                    Robert W. Ashton

Approved for public release; distribution is unlimited

94-08205

94 3 11 161

# REPORT DOCUMENTATION PAGE

| 1a. REPORT SECURITY CLASSIFICATION | | 1b. RESTRICTIVE MARKINGS | |
|---|---|---|---|
| UNCLASSIFIED | | | |
| 2a. SECURITY CLASSIFICATION AUTHORITY | | 3. DISTRIBUTION/AVAILABILITY OF REPORT | |
| | | Approved for public release; distribution is unlimited | |
| 2b. DECLASSIFICATION/DOWNGRADING SCHEDULE | | | |
| 4. PERFORMING ORGANIZATION REPORT NUMBER(S) | | 5. MONITORING ORGANIZATION REPORT NUMBER(S) | |
| 6a. NAME OF PERFORMING ORGANIZATION | 6b. OFFICE SYMBOL (If applicable) | 7a. NAME OF MONITORING ORGANIZATION | |
| Naval Postgraduate School | ECE | Naval Postgraduate School | |
| 6c. ADDRESS (City, State, and ZIP Code) | | 7b. ADDRESS (City, State, and ZIP Code) | |
| Monterey, CA 93943-5000 | | Monterey, CA 93943-5000 | |
| 8a. NAME OF FUNDING/SPONSORING ORGANIZATION | 8b. OFFICE SYMBOL (If applicable) | 9. PROCUREMENT INSTRUMENT IDENTIFICATION NUMBER | |
| 8c. ADDRESS (City, State, and ZIP Code) | | 10. SOURCE OF FUNDING NUMBERS | |

| | PROGRAM ELEMENT NO. | PROJECT NO. | TASK NO. | WORK UNIT ACCESSION NO. |
|---|---|---|---|---|
| | | | | |

**11. TITLE (Include Security Classification)**
GRAPHICAL MODELING OF SHIPBOARD ELECTRIC POWER DISTRIBUTION SYSTEMS

**12. PERSONAL AUTHOR(S)**
Kline, Daniel Bryan

| 13a. TYPE OF REPORT | 13b. TIME COVERED | 14. DATE OF REPORT (Year,Month,Day) | 15. PAGE COUNT |
|---|---|---|---|
| Masters Thesis | FROM ____ TO ____ | December 1993 | 74 |

**16. SUPPLEMENTARY NOTATION**
The views expressed in this thesis are those of the author and do not reflect the official policy or position of the Department of Defense or the U.S. Government.

| 17. COSATI CODES | | | 18. SUBJECT TERMS (Continue on reverse if necessary and identify by block number) |
|---|---|---|---|
| FIELD | GROUP | SUB-GROUP | Electric power systems, electric machine simulation, shipboard power systems, power system modelling |
| | | | |

**19. ABSTRACT (Continue on reverse if necessary and identify by block number)**

With the increasing application of power electronics to shipboard electric power systems, there is a need for studying power systems in an object-oriented, graphical environment in order to examine the interrelations of the various system components.

This thesis presents a method of analyzing shipboard electric power systems in a graphical environment. The simulation method used allows for real-time observation of the various power system measurements of interest.

The machine equations, including those for voltage, torque, and rotor angle are developed which permit analyzing the machine in any chosen reference frame depending on the study being undertaken. Regulators for both speed and field voltage are developed and the stability of the speed regulator is examined. A means of modeling a load for a synchronous generator is then shown which accurately interrelates the loading of the generator and the frequency and voltage output of the machine. This load is then connected to the synchronous generator and two different scenarios are examined including a fifty percent load change and a fault study. Graphs showing the output of these studies are presented.

| 20. DISTRIBUTION/AVAILABILITY OF ABSTRACT | 21. ABSTRACT SECURITY CLASSIFICATION | |
|---|---|---|
| [X] UNCLASSIFIED/UNLIMITED [ ] SAME AS RPT. [ ] DTIC USERS | Unclassified | |
| 22a. NAME OF RESPONSIBLE INDIVIDUAL | 22b. TELEPHONE (Include Area Code) | 22c. OFFICE SYMBOL |
| Ashton, Robert W. | 408-656-2928 | EC/AH |

# GRAPHICAL MODELING OF SHIPBOARD ELECTRIC POWER DISTRIBUTION SYSTEMS

by

**Daniel B. Kline**
Lieutenant, United States Navy
B.S., Oregon State University, 1987

Submitted in partial fulfillment of the
requirements for the degree of

## MASTER OF SCIENCE IN ELECTRICAL ENGINEERING

from the

## NAVAL POSTGRADUATE SCHOOL
December 1993

Author: _____
Daniel B. Kline

Approved by: _____
Robert W. Ashton, Thesis Advisor

_____
Harold A. Titus, Second Reader

_____
Michael A. Morgan, Chairman,
Department of Electrical and Computer Engineering

# ABSTRACT

With the increasing application of power electronics to shipboard electric power systems, there is a need for studying power systems in an object-oriented, graphical environment in order to examine the interrelations of the various system components.

This thesis presents a method of analyzing shipboard electric power systems in a graphical environment. The simulation method used allows for real-time observation of the various power system measurements of interest.

The machine equations, including those for voltage, torque, and rotor angle are developed which permit analyzing the machine in any chosen reference frame depending on the study being undertaken. Regulators for both speed and field voltage are developed and the stability of the speed regulator is examined. A means of modeling a load for a synchronous generator is then shown which accurately interrelates the loading of the generator and the frequency and voltage output of the machine. This load is then connected to the synchronous generator and two different scenarios are examined, including a fifty percent load change and a fault study. Graphs showing the output of these studies are presented.

# TABLE OF CONTENTS

# LIST OF FIGURES

# I. SYNCHRONOUS MACHINE MODEL DEVELOPMENT

The primary means of shipboard electric power generation is with synchronous generators driven by steam turbines. The electrical and electromechanical behavior of the synchronous generator can be accurately predicted from the equations for a three-phase salient-pole synchronous machine.

The rotor of the synchronous generator is equipped with a field winding and one or more damper windings. The rotor windings usually all have different electrical characteristics. Besides the differing electrical characteristics, the salient-pole machine exhibits a magnetically asymmetrical geometry due to the varying air-gap path for the magnetic flux. This magnetic asymmetry creates time-varying self- and mutual-inductance terms in the voltage equations for the stator variables. By transforming the equations into a reference frame which rotates at the same angular velocity as the rotor, the magnetic flux path remains constant, thereby eliminating the time-varying inductance terms.

This chapter develops the voltage and electromagnetic torque equations for the synchronous generator in terms of machine variables and then converts these equations to the rotor reference frame via Park's transformation [1]. The developed model assumes a magnetically linear system thereby neglecting the effects of saturation. Saturation could be accounted for with the addition of another simulation segment for the model, however saturation data for the machines studied was unavailable.

1

## A. VOLTAGE EQUATIONS IN MACHINE VARIABLES

Voltage equations for the synchronous generator will be developed from a simple two-pole, three-phase, wye-connected, salient-pole synchronous machine shown in Figure 1. The number of poles of the particular machine can be easily changed as this is one of the variables of the resulting torque equations. The stator windings are assumed identical with sinusoidally distributed windings, displaced 120°, with $N_S$ equivalent turns and equivalent resistance $r_S$ (subscript $s$ denoting stator variables). A field winding and three damper windings (*fd*, *kd*, *kq1*, and *kq2* respectively) are installed on the rotor. All windings are assumed sinusoidal with applicable $N$ equivalent turns and resistance $r$ (subscript denoting particular circuit). The quadrature axis (*q* axis) and direct axis (*d* axis) are used with reference to the magnetic axis of the rotor circuits. Voltages of the rotor damper windings ($v_{kd}$, $v_{kq1}$, and $v_{kq2}$) are for monitoring purposes only, the windings themselves are physically shorted.

Voltage equations in machine variables [2] may be expressed in matrix form as

$$\mathbf{v}_{abcs} = -\mathbf{r}_s \mathbf{i}_{abcs} + p\lambda_{abcs} \tag{1}$$

$$\mathbf{v}_{qdr} = \mathbf{r}_r \mathbf{i}_{qdr} + p\lambda_{qdr} \tag{2}$$

where

$$\begin{bmatrix} \lambda_{abcs} \\ \lambda_{qdr} \end{bmatrix} = \begin{bmatrix} \mathbf{L}_s & \mathbf{L}_{sr} \\ (\mathbf{L}_{sr})^T & \mathbf{L}_r \end{bmatrix} \begin{bmatrix} -\mathbf{i}_{abcs} \\ \mathbf{i}_{qdr} \end{bmatrix} \tag{3}$$
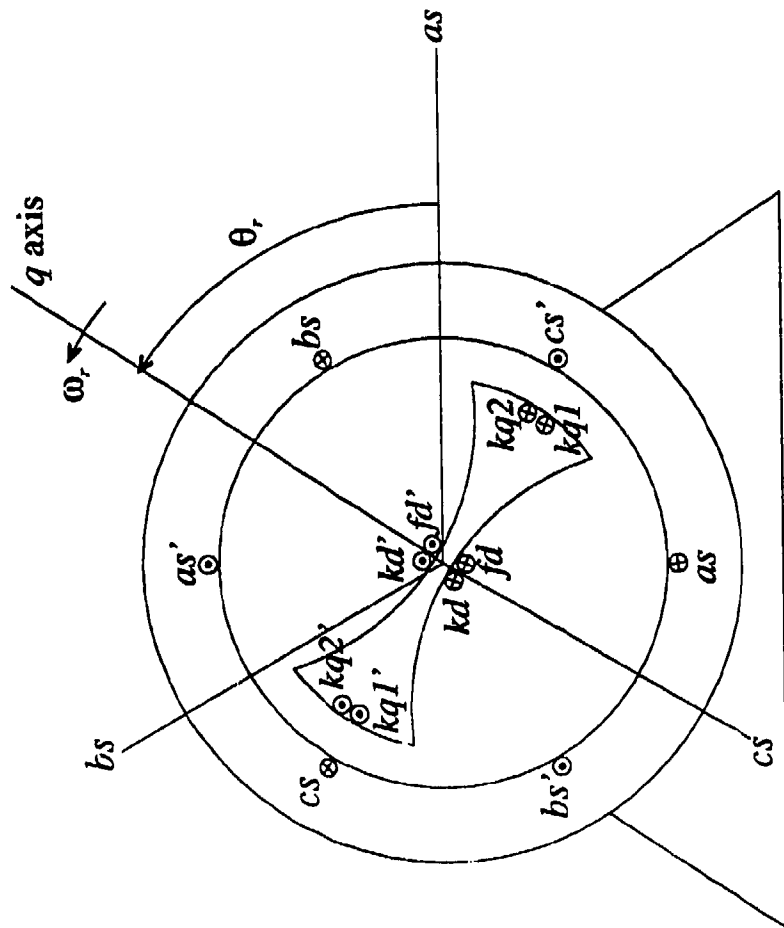
**Figure 1. 2-Pole, 3-Phase Synchronous Machine.**

3

and

$$\mathbf{L}_s = \begin{bmatrix} L_{ls} + L_A - L_B \cos 2\theta_r & -\dfrac{1}{2} L_A - L_B \cos 2(\theta_r - \dfrac{\pi}{3}) & -\dfrac{1}{2} L_A - L_B \cos 2(\theta_r + \dfrac{\pi}{3}) \\ -\dfrac{1}{2} L_A - L_B \cos 2(\theta_r - \dfrac{\pi}{3}) & L_{ls} + L_A - L_B \cos 2(\theta_r - \dfrac{2\pi}{3}) & -\dfrac{1}{2} L_A - L_B \cos 2(\theta_r + \pi) \\ -\dfrac{1}{2} L_A - L_B \cos 2(\theta_r + \dfrac{\pi}{3}) & -\dfrac{1}{2} L_A - L_B \cos 2(\theta_r + \pi) & L_{ls} + L_A - L_B \cos 2(\theta_r + \dfrac{2\pi}{3}) \end{bmatrix} \tag{4}$$

$$\mathbf{L}_{sr} = \begin{bmatrix} L_{skq1} \cos\theta_r & L_{skq2} \cos\theta_r & L_{sfd} \sin\theta_r & L_{skd} \sin\theta_r \\ L_{skq1} \cos(\theta_r - \dfrac{2\pi}{3}) & L_{skq2} \cos(\theta_r - \dfrac{2\pi}{3}) & L_{sfd} \sin(\theta_r - \dfrac{2\pi}{3}) & L_{skd} \sin(\theta_r - \dfrac{2\pi}{3}) \\ L_{skq1} \cos(\theta_r + \dfrac{2\pi}{3}) & L_{skq2} \cos(\theta_r + \dfrac{2\pi}{3}) & L_{sfd} \sin(\theta_r + \dfrac{2\pi}{3}) & L_{skd} \sin(\theta_r + \dfrac{2\pi}{3}) \end{bmatrix} \tag{5}$$

$$\mathbf{L}_r = \begin{bmatrix} L_{lkq1} + L_{mkq1} & L_{kq1kq2} & 0 & 0 \\ L_{kq1kq2} & L_{lkq2} + L_{mkq2} & 0 & 0 \\ 0 & 0 & L_{lfd} + L_{mfd} & L_{fdkd} \\ 0 & 0 & L_{fdkd} & L_{lkd} + L_{mkd} \end{bmatrix} \tag{6}$$

In (1) and (2), the time differential operator is $p$. In (4) and (6), the subscript $l$ denotes a leakage inductance term. The subscripts $skq1$, $skq2$, $sfd$, and $skd$ denote mutual inductances between stator and rotor windings.

The magnetizing inductances are defined as

$$L_{mq} = \frac{3}{2}(L_A - L_B) \tag{7}$$

$$L_{md} = \frac{3}{2}(L_A + L_B) \tag{8}$$

where the term incorporating $L_A$ refers to the inductance term which is independent of rotor position and the term with $L_B$ is the inductance term which is position dependent.

The rotor variables are then referred to the stator windings via the appropriate turns ratio giving the following equations

$$
\begin{bmatrix} \lambda_{abcs} \\ \lambda'_{qdr} \end{bmatrix} = \begin{bmatrix} \mathbf{L}_s & \mathbf{L}'_{sr} \\ \frac{2}{3}(\mathbf{L}'_{sr})^T & \mathbf{L}'_r \end{bmatrix} \begin{bmatrix} -\mathbf{i}_{rbcs} \\ \mathbf{i}'_{qdr} \end{bmatrix}
$$
(9)

$$
\mathbf{L}'_{sr} = \begin{bmatrix}
L_{mq}\cos\theta_r & L_{mq}\cos\theta_r & L_{md}\sin\theta_r & L_{md}\sin\theta_r \\
L_{mq}\cos(\theta_r - \frac{2\pi}{3}) & L_{mq}\cos(\theta_r - \frac{2\pi}{3}) & L_{md}\sin(\theta_r - \frac{2\pi}{3}) & L_{md}\sin(\theta_r - \frac{2\pi}{3}) \\
L_{mq}\cos(\theta_r + \frac{2\pi}{3}) & L_{mq}\cos(\theta_r + \frac{2\pi}{3}) & L_{md}\sin(\theta_r + \frac{2\pi}{3}) & L_{md}\sin(\theta_r + \frac{2\pi}{3})
\end{bmatrix}
$$
(10)

$$
\mathbf{L}'_r = \begin{bmatrix}
L'_{lkq1} + L_{mq} & L_{mq} & 0 & 0 \\
L_{mq} & L'_{lkq2} + L_{mq} & 0 & 0 \\
0 & 0 & L'_{lfd} + L_{md} & L_{md} \\
0 & 0 & L_{md} & L'_{lkd} + L_{md}
\end{bmatrix}
$$
(11)

where the primed variables (i.e. $\mathbf{L}'_{sr}$) refer the appropriate rotor variable to the stator windings.

The voltage equations expressed in terms of machine variables referred to the stator windings are

$$
\begin{bmatrix} \mathbf{v}_{abcs} \\ \mathbf{v}'_{qdr} \end{bmatrix} = \begin{bmatrix} \mathbf{r}_s + p\mathbf{L}_s & p\mathbf{L}'_{sr} \\ \frac{2}{3}p(\mathbf{L}'_{sr})^T & \mathbf{r}'_r + p\mathbf{L}'_r \end{bmatrix} \begin{bmatrix} -\mathbf{i}_{abcs} \\ \mathbf{i}'_{qdr} \end{bmatrix}
$$
(12)

Note that the voltage equations (12) are valid for positive direction of stator current assumed out of the stator terminals. If motor action is assumed, the sign preceding $\mathbf{i}_{abcs}$ must be changed.

5

## B. TORQUE EQUATION IN MACHINE VARIABLES

The field energy stored in the coupling field of a synchronous machine can be expressed as

$$W_f = \frac{1}{2} (\mathbf{i}_{abcs})^T (\mathbf{L}_s - L_{ls}\mathbf{I})\mathbf{i}_{abcs} - (\mathbf{i}_{abcs})^T \mathbf{L}'_{sr}\mathbf{i}'_{qdr}$$
$$+ \frac{1}{2} (\frac{3}{2})(\mathbf{i}'_{qdr})^T (\mathbf{L}'_r - L'_{lr}\mathbf{I})\mathbf{i}'_{qdr} \qquad (13)$$

where

$$\mathbf{L}'_{lr} = \text{diag}\begin{bmatrix} L'_{lkq1} & L'_{lkq2} & L'_{lfd} & L'_{lkd} \end{bmatrix} \qquad (14)$$

The electromagnetic torque is found by taking the partial derivative of the coenergy with respect to the rotor angular displacement $\theta_r$. The magnetic system is assumed linear, therefore the coenergy equals the field energy, and upon taking the partial derivative, the electrical torque is

$$T_e = (\frac{P}{2})\left\{ -\frac{1}{2}(\mathbf{i}_{abcs})^T \frac{\partial}{\partial\theta_r}[\mathbf{L}_s - L_{ls}\mathbf{I}]\mathbf{i}_{abcs} + (\mathbf{i}_{abcs})^T \frac{\partial}{\partial\theta_r}[\mathbf{L}'_{sr}]\mathbf{i}'_{qdr} \right\} \qquad (15)$$

where $P$ is the number of poles of the machine. The torque is positive for generator action with the positive direction of stator current assumed out of the stator terminals.

The torque and rotor speed are related by

$$T_e = -J(\frac{2}{P})p\omega_r + T_l \qquad (16)$$

6

where $J$ is the inertia of the machine in kilogram meters$^2$ (kg·m$^2$) or Joule seconds$^2$ (J·s$^2$). The input torque $T_I$ is positive for a torque applied to the shaft of the synchronous machine.

## C.  VOLTAGE EQUATIONS IN THE ROTOR REFERENCE-FRAME

The machine voltage equations (1) and (2) are seen to contain flux-linkage terms which are dependent on rotor position $\theta_r$. The analysis of the machine behavior is greatly simplified by transforming these time-varying inductances to constant inductance terms. This can be realized if the stator variables are transformed to the rotor reference frame. R.H. Park was the first to incorporate a change of variables in the analysis of synchronous machines [1].

A change of variables which formulates a transformation of the 3-phase variables of the stationary circuit elements (thus the need to refer the rotor variables to the stator) to the rotor reference frame may be expressed as

$$\mathbf{f}_{qd0s} = \mathbf{K}_s^r \mathbf{f}_{abcs} \tag{17}$$

where

$$\mathbf{f}_{qd0s} = \begin{bmatrix} f_{qs} \\ f_{ds} \\ f_{0s} \end{bmatrix} \tag{18}$$

7

$$\mathbf{f}_{abcs} = \begin{bmatrix} f_{as} \\ f_{bs} \\ f_{cs} \end{bmatrix} \tag{19}$$

and

$$\mathbf{K}_s^r = \frac{2}{3} \begin{bmatrix} \cos\theta_r & \cos(\theta_r - \frac{2\pi}{3}) & \cos(\theta_r + \frac{2\pi}{3}) \\ \sin\theta_r & \sin(\theta_r - \frac{2\pi}{3}) & \sin(\theta_r + \frac{2\pi}{3}) \\ \frac{1}{2} & \frac{1}{2} & \frac{1}{2} \end{bmatrix} \tag{20}$$

$$\theta_r = \int_0^t \omega_r(\xi)\, d\xi + \theta_r(0) \tag{21}$$

The term $\mathbf{K}_s^r$ denotes the transformation matrix of stator variables (the subscript-$s$) to the rotor reference frame (the superscript-$r$). It can be shown that the voltage equations (1) and (2) are transformed into

$$\mathbf{v}_{qd0s}^r = -\mathbf{r}_s \mathbf{i}_{qd0s}^r + \omega_r \lambda_{dqs}^r + p\lambda_{qd0s}^r \tag{22}$$

$$\mathbf{v}_{qdr}^{\prime r} = \mathbf{r}_r^{\prime} \mathbf{i}_{qdr}^{\prime r} + p\lambda_{qdr}^{\prime r} \tag{23}$$

where

$$(\lambda_{dqs}^{r}) = \begin{bmatrix} \lambda_{ds}^{r} \\ -\lambda_{qs}^{r} \\ 0 \end{bmatrix} \tag{24}$$

8

The flux-linkages can be expressed in the rotor reference frame by transforming (9) to obtain

$$
\begin{bmatrix} \lambda^r_{qd0s} \\ \lambda'^{\,r}_{qdr} \end{bmatrix} = \begin{bmatrix} \mathbf{K}^r_s \mathbf{L}_s (\mathbf{K}^r_s)^{-1} & \mathbf{K}^r_s \mathbf{L}'_{sr} \\ \dfrac{2}{3} (\mathbf{L}'_{sr})^T (\mathbf{K}^r_s)^{-1} & \mathbf{L}'_r \end{bmatrix} \begin{bmatrix} -\mathbf{i}^r_{qd0s} \\ \mathbf{i}''^{\,r}_{qdr} \end{bmatrix}
\tag{25}
$$

Expanding the voltage equations given by (22) and (23) gives

$$
v^r_{qs} = -r_s i^r_{qs} + \omega_r \lambda^r_{ds} + p\lambda^r_{qs}
\tag{26}
$$

$$
v^r_{ds} = -r_s i^r_{ds} - \omega_r \lambda^r_{qs} + p\lambda^r_{ds}
\tag{27}
$$

$$
v_{0s} = -r_s i_{0s} + p\lambda_{0s}
\tag{28}
$$

$$
v''^{\,r}_{kq1} = r'_{kq1} i''^{\,r}_{kq1} + p\lambda''^{\,r}_{kq1}
\tag{29}
$$

$$
v''^{\,r}_{kq2} = r'_{kq2} i''^{\,r}_{kq2} + p\lambda''^{\,r}_{kq2}
\tag{30}
$$

$$
v''^{\,r}_{fd} = r'_{fd} i''^{\,r}_{fd} + p\lambda''^{\,r}_{fd}
\tag{31}
$$

$$
v''^{\,r}_{kd} = r'_{kd} i''^{\,r}_{kd} + p\lambda''^{\,r}_{kd}
\tag{32}
$$

and the expanded flux linkage terms become

$$
\lambda^r_{qs} = -L_{ls} i^r_{qs} + L_{mq} (-i^r_{qs} + i''^{\,r}_{kq1} + i''^{\,r}_{kq2})
\tag{33}
$$

$$
\lambda^r_{ds} = -L_{ls} i^r_{ds} + L_{md} (-i^r_{ds} + i''^{\,r}_{kd} + i''^{\,r}_{fd})
\tag{34}
$$

$$
\lambda_{0s} = -L_{ls} i_{0s}
\tag{35}
$$

$$
\lambda'^{\,r}_{kq1} = L'_{lkq1} i''^{\,r}_{kq1} + L_{mq} (-i^r_{qs} + i''^{\,r}_{kq1} + i''^{\,r}_{kq2})
\tag{36}
$$

$$
\lambda'^{\,r}_{kq2} = L'_{lkq2} i''^{\,r}_{kq2} + L_{mq} (-i^r_{qs} + i''^{\,r}_{kq1} + i''^{\,r}_{kq2})
\tag{37}
$$

$$
\lambda'^{\,r}_{fd} = L'_{lfd} i''^{\,r}_{fd} + L_{md} (-i^r_{ds} + i''^{\,r}_{fd} + i''^{\,r}_{kd})
\tag{38}
$$

$$
\lambda'^{\,r}_{kd} = L'_{lkd} i''^{\,r}_{kd} + L_{md} (-i^r_{ds} + i''^{\,r}_{fd} + i''^{\,r}_{kd})
\tag{39}
$$

9

Expressing the voltage and flux linkage equations in terms of reactances rather than inductances gives the voltage equations in matrix format (40), where the expression for the applied field voltage is introduced

$$e''_{xfd} = v''_{fd} \frac{X_{md}}{r'_{fd}} \tag{41}$$

and the leakage and magnetic reactances are combined as

$$X_q = X_{ls} + X_{mq} \tag{42}$$

$$X_d = X_{ls} + X_{md} \tag{43}$$

$$X'_{kq1} = X'_{lkq1} + X_{mq} \tag{44}$$

$$X'_{kq2} = X'_{lkq2} + X_{mq} \tag{45}$$

$$X'_{fd} = X'_{lfd} + X_{md} \tag{46}$$

$$X'_{kd} = X'_{lkd} + X_{md} \tag{47}$$

The zero sequence terms have been omitted since balanced conditions are assumed.

The model being developed will be connected to a non-infinite bus. This implies that the voltage and frequency do indeed vary with load, based on the droop characteristics of the particular regulator. With this in mind, it is necessary to solve for currents based on the bus voltages, therefore the c rrents are selected as independent variables. Rewriting (40) with the current and current derivative terms separated.

10

$$
\begin{bmatrix}
v_{qs}^r \\
v_{ds}^r \\
v_{kq1}^{rr} \\
v_{kq2}^{rr} \\
e_{xfd}^{rr} \\
v_{kd}^{rr}
\end{bmatrix}
=
\begin{bmatrix}
-r_s - \dfrac{p}{\omega_b}X_q & -\dfrac{\omega_r}{\omega_b}X_d & \dfrac{p}{\omega_b}X_{mq} & \dfrac{p}{\omega_b}X_{mq} & \dfrac{\omega_r}{\omega_b}X_{md} & \dfrac{\omega_r}{\omega_b}X_{md} \\[2ex]
\dfrac{\omega_r}{\omega_b}X_q & -r_s-\dfrac{p}{\omega_b}X_d & \dfrac{\omega_r}{\omega_b}X_{mq} & \dfrac{\omega_r}{\omega_b}X_{mq} & \dfrac{p}{\omega_b}X_{md} & \dfrac{p}{\omega_b}X_{md} \\[2ex]
-\dfrac{p}{\omega_b}X_{mq} & 0 & r'_{kq1}+\dfrac{p}{\omega_b}X'_{kq1} & \dfrac{p}{\omega_b}X_{mq} & 0 & 0 \\[2ex]
-\dfrac{p}{\omega_b}X_{mq} & 0 & \dfrac{p}{\omega_b}X_{mq} & r'_{kq2}+\dfrac{p}{\omega_b}X'_{kq2} & 0 & 0 \\[2ex]
0 & -\dfrac{X_{md}}{r'_{fd}}\left(\dfrac{p}{\omega_b}X_{md}\right) & 0 & 0 & \dfrac{X_{md}}{r'_{fd}}\left(r'_{fd}+\dfrac{p}{\omega_b}X'_{fd}\right) & \dfrac{X_{md}}{r'_{fd}}\left(\dfrac{p}{\omega_b}X_{md}\right) \\[2ex]
0 & -\dfrac{p}{\omega_b}X_{md} & 0 & 0 & \dfrac{p}{\omega_b}X_{md} & r'_{kd}+\dfrac{p}{\omega_b}X'_{kd}
\end{bmatrix}
\begin{bmatrix}
i_{qs}^r \\
i_{ds}^r \\
i_{kq1}^{rr} \\
i_{kq2}^{rr} \\
i_{fd}^{rr} \\
i_{kd}^{rr}
\end{bmatrix}
\tag{40}
$$

11

$$
\begin{bmatrix} v_{qs}^r \\ v_{ds}^r \\ v_{kq1}''^r \\ v_{kq2}''^r \\ e_{xkd}''^r \\ v_{kd}''^r \end{bmatrix}
=
\begin{bmatrix}
-r_s & -\dfrac{\omega_r}{\omega_b}X_d & 0 & 0 & \dfrac{\omega_r}{\omega_b}X_{md} & \dfrac{\omega_r}{\omega_b}X_{md} \\[2mm]
\dfrac{\omega_r}{\omega_b}X_q & -r_s & -\dfrac{\omega_r}{\omega_b}X_{mq} & -\dfrac{\omega_r}{\omega_b}X_{mq} & 0 & 0 \\[2mm]
0 & 0 & r_{kq1}' & 0 & 0 & 0 \\[2mm]
0 & 0 & 0 & r_{kq2}' & 0 & 0 \\[2mm]
0 & 0 & 0 & 0 & X_{md} & 0 \\[2mm]
0 & 0 & 0 & 0 & 0 & r_{kd}'
\end{bmatrix}
\begin{bmatrix} i_{qs}^r \\ i_{ds}^r \\ i_{kq1}''^r \\ i_{ks2}''^r \\ i_{fd}''^r \\ i_{kd}''^r \end{bmatrix}
$$

$$
+
\begin{bmatrix}
-\dfrac{X_q}{\omega_b} & 0 & \dfrac{X_{mq}}{\omega_b} & \dfrac{X_{mq}}{\omega_b} & 0 & 0 \\[3mm]
0 & -\dfrac{X_d}{\omega_b} & 0 & 0 & \dfrac{X_{md}}{\omega_b} & \dfrac{X_{md}}{\omega_b} \\[3mm]
-\dfrac{X_{mq}}{\omega_b} & 0 & \dfrac{X_{kq1}'}{\omega_b} & \dfrac{X_{mq}}{\omega_b} & 0 & 0 \\[3mm]
-\dfrac{X_{mq}}{\omega_b} & 0 & \dfrac{X_{mq}}{\omega_b} & \dfrac{X_{kq2}'}{\omega_b} & 0 & 0 \\[3mm]
0 & -\dfrac{X_{md}}{r_{fd}'}\dfrac{X_{md}}{\omega_b} & 0 & 0 & \dfrac{X_{md}}{r_{fd}'}\dfrac{X_{fd}'}{\omega_b} & \dfrac{X_{md}}{r_{fd}'}\dfrac{X_{md}}{\omega_b} \\[3mm]
0 & -\dfrac{X_{md}}{\omega_b} & 0 & 0 & \dfrac{X_{md}}{\omega_b} & \dfrac{X_{kd}'}{\omega_b}
\end{bmatrix}
\begin{bmatrix} pi_{qs}^r \\ pi_{ds}^r \\ pi_{kq1}''^r \\ pi_{ks2}''^r \\ pi_{fd}''^r \\ pi_{kd}''^r \end{bmatrix}
$$

(48)

The state equation format of (48) is used for the simulation, so the current derivatives must be solved for. As an example

$$
\begin{aligned}
v &= [A]i + [B]p\,i \\
p\,i &= [B]^{-1}\{v - [A]i\}
\end{aligned}
$$

(49)

and, with this format, the current derivatives are solved as shown in (50)

12

$$
\begin{bmatrix} pi^{r}_{qs} \\ pi^{r}_{ds} \\ pi''^{r}_{kq1} \\ pi''^{r}_{kq2} \\ pi'^{r}_{fd} \\ pi''^{r}_{kd} \end{bmatrix}
=
\begin{bmatrix}
-\dfrac{X_q}{\omega_b} & 0 & -\dfrac{X_{mq}}{\omega_b} & -\dfrac{X_{mq}}{\omega_b} & 0 & 0 \\[6pt]
0 & -\dfrac{X_d}{\omega_b} & 0 & 0 & -\dfrac{X_{md}}{r'_{fd}}\dfrac{X_{md}}{\omega_b} & -\dfrac{X_{md}}{\omega_b} \\[6pt]
\dfrac{X_{mq}}{\omega_b} & 0 & \dfrac{X'_{kq1}}{\omega_b}\,\dfrac{X_{mq}}{\omega_b} & \dfrac{X_{mq}}{\omega_b} & 0 & 0 \\[6pt]
\dfrac{X_{mq}}{\omega_b} & 0 & \dfrac{X_{mq}}{\omega_b}\,\dfrac{X'_{kq2}}{\omega_b} & \dfrac{X_{mq}}{\omega_b} & 0 & 0 \\[6pt]
0 & \dfrac{X_{md}}{\omega_b} & 0 & 0 & \dfrac{X_{md}}{r'_{fd}}\dfrac{X'_{fd}}{\omega_b}\,\dfrac{X_{md}}{\omega_b} & \dfrac{X_{md}}{\omega_b} \\[6pt]
0 & \dfrac{X_{md}}{\omega_b} & 0 & 0 & \dfrac{X_{md}}{r'_{fd}}\dfrac{X'_{kd}}{\omega_b}\,\omega_b & \dfrac{X_{md}}{\omega_b}
\end{bmatrix}^{-1}
*
$$

$$
\left(
\begin{bmatrix} v^{r}_{qs} \\ v^{r}_{ds} \\ v''^{r}_{kq1} \\ v''^{r}_{kq2} \\ e'^{r}_{xfd} \\ v''^{r}_{kd} \end{bmatrix}
-
\begin{bmatrix}
-r_s & \dfrac{\omega_r}{\omega_b}X_q & 0 & 0 & 0 & 0 \\[4pt]
-\dfrac{\omega_r}{\omega_b}X_d & -r_s & 0 & 0 & 0 & 0 \\[4pt]
0 & 0 & r'_{kq1} & 0 & 0 & 0 \\[4pt]
-\dfrac{\omega_r}{\omega_b}X_{mq} & 0 & 0 & r'_{kq2} & 0 & 0 \\[4pt]
0 & \dfrac{\omega_r}{\omega_b}X_{md} & 0 & 0 & X_{md} & 0 \\[4pt]
\dfrac{\omega_r}{\omega_b}X_{md} & 0 & 0 & 0 & 0 & r'_{kd}
\end{bmatrix}
\begin{bmatrix} i^{r}_{qs} \\ i^{r}_{ds} \\ i''^{r}_{kq1} \\ i''^{r}_{kq2} \\ i'^{r}_{fd} \\ i''^{r}_{kd} \end{bmatrix}
\right)
$$

(50)

13

Denoting the inverse matrix elements as $[\mathbf{B}]^{-1} = [\mathbf{b}] = \begin{bmatrix} b_{11} & b_{12} & \cdot & \cdot & \cdot \\ b_{21} & \cdot & \cdot & \cdot & \\ \cdot & \cdot & \cdot & & \\ \cdot & & & & \\ \cdot & & & & \\ b_{61} & & \cdot & \cdot & \cdot & b_{66} \end{bmatrix}$

the desired differential current equations are obtained

$$pi_{q_s}^r = b_{11}[v_{qs}^r + r_s i_{qs}^r + \omega_r \frac{X_d}{\omega_b} i_{ds}^r - \omega_r \frac{X_{md}}{\omega_b} i_{fd}''^r - \omega_r \frac{X_{md}}{\omega_b} i_{kd}''^r]$$

$$+ b_{13}[v_{kq1}''^r - r_{kq1}' i_{kq1}''^r]$$ 

$$+ b_{14}[v_{kq2}''^r - r_{kq2}' i_{kq2}''^r]$$

(51)

$$pi_{kq1}''^r = b_{31}[v_{qs}^r + r_s i_{qs}^r + \omega_r \frac{X_d}{\omega_b} i_{ds}^r - \omega_r \frac{X_{md}}{\omega_b} i_{fd}''^r - \omega_r \frac{X_{md}}{\omega_b} i_{kd}''^r]$$

$$+ b_{33}[v_{kq1}''^r - r_{kq1}' i_{kq1}''^r]$$

$$+ b_{34}[v_{kq2}''^r - r_{kq2}' i_{kq2}''^r]$$

(52)

$$pi_{kq2}''^r = b_{41}[v_{qs}^r + r_s i_{qs}^r + \omega_r \frac{X_d}{\omega_b} i_{ds}^r - \omega_r \frac{X_{md}}{\omega_b} i_{fd}''^r - \omega_r \frac{X_{md}}{\omega_b} i_{kd}''^r]$$

$$+ b_{43}[v_{kq1}''^r - r_{kq1}' i_{kq1}''^r]$$

$$+ b_{44}[v_{kq2}''^r - r_{kq2}' i_{kq2}''^r]$$

(53)

$$pi_{ds}^r = b_{22}[v_{ds}^r + r_s i_{ds}^r - \omega_r \frac{X_q}{\omega_b} i_{qs}^r + \omega_r \frac{X_{mq}}{\omega_b} i_{kq1}''^r + \omega_r \frac{X_{mq}}{\omega_b} i_{kq2}''^r]$$

$$+ b_{25}[e_{xfd}''^r - X_{md} i_{fd}^r]$$

$$+ b_{26}[v_{kd}''^r - r_{kd}' i_{kd}''^r]$$

(54)

14

$$pi_{fd}^{\prime\prime r} = b_{52}[v_{ds}^r + r_s i_{ds}^r - \omega_r \frac{X_q}{\omega_b} i_{qs}^r + \omega_r \frac{X_{mq}}{\omega_b} i_{kq1}^{\prime\prime r} + \omega_r \frac{X_{mq}}{\omega_b} i_{kq2}^{\prime\prime r}]$$

$$+ b_{55}[e_{xfd}^{\prime\prime r} - X_{md} i_{fd}^r] \tag{55}$$

$$+ b_{56}[v_{kd}^{\prime\prime r} - r_{kd}^\prime i_{kd}^{\prime\prime r}]$$

$$pi_{kd}^{\prime\prime r} = b_{62}[v_{ds}^r + r_s i_{ds}^r - \omega_r \frac{X_q}{\omega_b} i_{qs}^r + \omega_r \frac{X_{mq}}{\omega_b} i_{kq1}^{\prime\prime r} + \omega_r \frac{X_{mq}}{\omega_b} i_{kq2}^{\prime\prime r}]$$

$$+ b_{65}[e_{xfd}^{\prime\prime r} - X_{md} i_{fd}^r] \tag{56}$$

$$+ b_{66}[v_{kd}^{\prime\prime r} - r_{kd}^\prime i_{kd}^{\prime\prime r}]$$

Note the similar form of the $q$- and the $d$-axis integral current equations. These will greatly simplify the SIMULINK [3] model.

## D TORQUE EQUATION IN SUBSTITUTE VARIABLES

The torque equation (15), transformed into rotor reference frame variables is

$$T_e = (\frac{3}{2})(\frac{P}{2})[L_{md}(-i_{ds}^r + i_{fd}^{\prime\prime r} + i_{kd}^{\prime\prime r})i_{qs}^r - L_{mq}(-i_{qs}^r + i_{kq1}^{\prime\prime r} + i_{kq2}^{\prime\prime r})i_{ds}^r] \tag{57}$$

and writing in terms of reactance

$$\frac{\omega_b L}{\omega_b} = \frac{X}{\omega_b} \Rightarrow L_{md} = \frac{X_{md}}{\omega_b} \text{ and } L_{mq} = \frac{X_{mq}}{\omega_b} \tag{58}$$

gives

$$T_e = (\frac{3}{2})(\frac{P}{2})[\frac{X_{md}}{\omega_b}(-i_{ds}^r + i_{fd}^{\prime\prime r} + i_{kd}^{\prime\prime r})i_{qs}^r - \frac{X_{mq}}{\omega_b}(-i_{qs}^r + i_{kq1}^{\prime\prime r} + i_{kq2}^{\prime\prime r})i_{ds}^r]$$ (59)

The rotor speed is obtained from (16) as

$$p\omega_r = (-\frac{P}{2J})(T_e - T_l)$$ (60)

## E. ROTOR ANGLE

The rotor angle of a synchronous machine is a useful parameter to monitor the torque production of the machine. It relates the angular displacement of the rotor and stator magneto motive force axes. In equation form

$$\begin{aligned}
\delta &= \theta_r - \theta_{ev} \\
&= \int_0^t [\omega_r(\xi) - \omega_{ev}(\xi)]d\xi + \theta_r(0) - \theta_{ev}(0)
\end{aligned}$$ (61)

where $\delta$ is the rotor angle (in radians), and $\xi$ is a dummy variable of integration.

Equation (61) can be implemented by solving equation (61) in terms of the available parameters. The rotor position, $\theta_r$, is available by integrating the rotor speed. However, the voltage angle $\theta_{ev}$ must be solved for as follows

$$\theta_{ev} = \int_0^t \omega_{ev}(\xi) \, d\xi + \theta_{ev}(0)$$ (62)

16

and

$$v_{as} = v_{qs} \cos \theta_r + v_{ds} \sin \theta_r$$

$$= \sqrt{v_{qs}^2 + v_{ds}^2} \cos[\theta_r + \tan^{-1}(\frac{v_{ds}}{v_{qs}})]$$

$$= \sqrt{v_{qs}^2 + v_{ds}^2} \cos[\underbrace{\int \omega_r \, dt + \theta_r(0) + \tan^{-1}(\frac{v_{ds}}{v_{qs}})}_{\theta_{ev}}]$$

(63)

therefore, from (62)

$$\theta_{ev} = \int_0^t \omega_{ev}(\xi) \, d\xi + \theta_{ev}(0)$$

$$= \underbrace{\int \omega_r \, dt + \theta_r(0)}_{\theta_r} + \tan^{-1}(\frac{v_{ds}}{v_{qs}})$$

(64)

giving

$$\delta = \theta_r - \theta_{ev} = \tan^{-1}(\frac{v_{ds}}{v_{qs}})$$

(65)

where a positive rotor angle is assumed for generator action.

## II.    SPEED AND VOLTAGE REGULATORS

For the machine model to accurately simulate a shipboard power system it is necessary to include controllers for both the field voltage and the prime mover torque. The two principal controllers of a turbine generator set are the automatic voltage regulator and the speed governor. The automatic voltage regulator model consists of voltage sensing equipment, comparators and amplifiers controlling a synchronous machine which can be generating or motoring. The speed governor may be considered to have similar equipment but in addition it is necessary to take the turbine into account.

### A.  SPEED REGULATOR

#### 1.   Model Development

The block diagram of a steam turbine and associated governor for a typical naval ship's service turbine generator (SSTG) is shown in Figure 2 [4].

The reference speed input is the no-load frequency selected by the operator of the electric plant. The gain K is used to adjust the speed droop of the regulator. $\tau_s$ is the time constant associated with the servo and steam valve system and $\tau_p$ is the time constant associated with the conversion of steam to torque ($T_{pm}$). The following values were used for this study

| | |
|---|---|
| $\tau_s$ | 0.1 sec |
| $\tau_p$ | 0.06 sec |
| K | 150 |

From this block diagram (Figure 2), a SIMULINK model was developed and is shown in Figure 3.

18
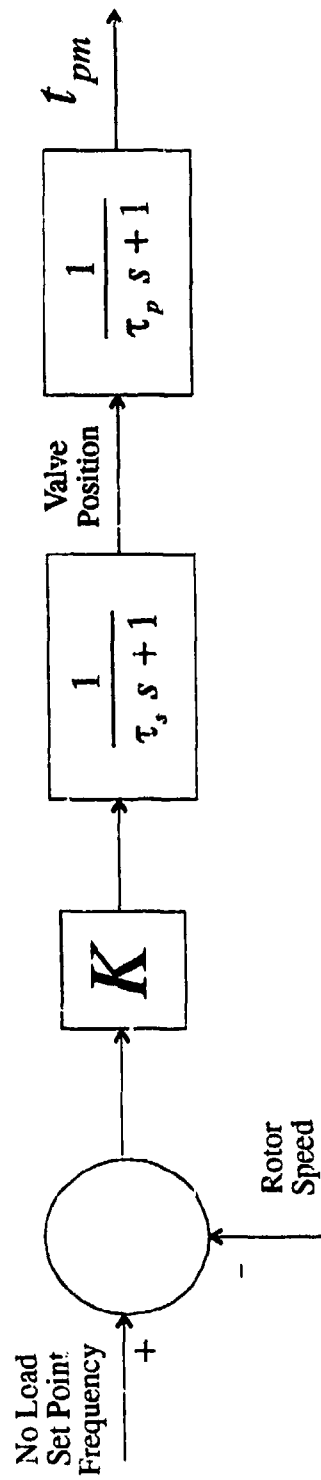
Figure 2. Block Diagram, Steam Turbine & Governor.
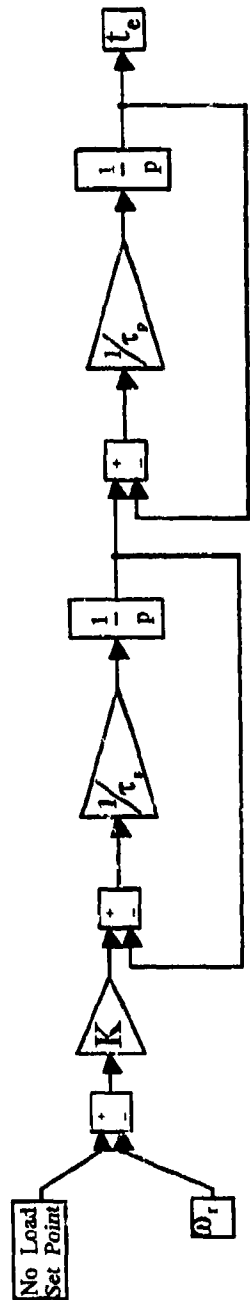
Figure 3. SIMULINK Speed Regulator.

20

As can be seen, the speed regulator is designed to compare the reference speed with the speed being produced by the synchronous machine. This speed difference determines the prime mover torque being applied to the generator. When the speed difference is no longer changing, the prime mover torque is equal to the electrical torque developed by the generator (load dependent). The final machine speed (and therefore the machine output frequency) will be at some value below the no-load set-point frequency. This can be demonstrated by referring to the 'house' diagram shown in Figure 4.

As the output power of the machine is increased, the operating frequency of the machine decreases (based on the slope or droop of the particular regulator) the operating frequency can be restored to a desired frequency (i.e., 60 Hz) by the operator adjusting the no-load setpoint of the regulator.

## 2. Regulator Stability

As was mentioned in the previous section, the speed droop characteristics of the regulator are determined by the gain K of the regulator. The percent speed regulation is defined by

$$\% \text{ Speed Regulation } = \frac{\omega_{nl} - \omega_{fl}}{\omega_{fl}} 100\% \qquad (62)$$

As the gain $K$ is raised, the percent speed regulation approaches 100%, at which point the regulator and therefore the regulated plant will become unstable. This stability point was determined by examining the root locus of the model of Figure 3. The synchronous machine model was obtained by linearizing the machines current block around its stable operating point for rated conditions by using the MATLAB [5] function *linmod*. The linearized plant model returned by *linmod* is in linearized state space format which is then changed to transfer function format with the function *ss2tf*. The transfer

21
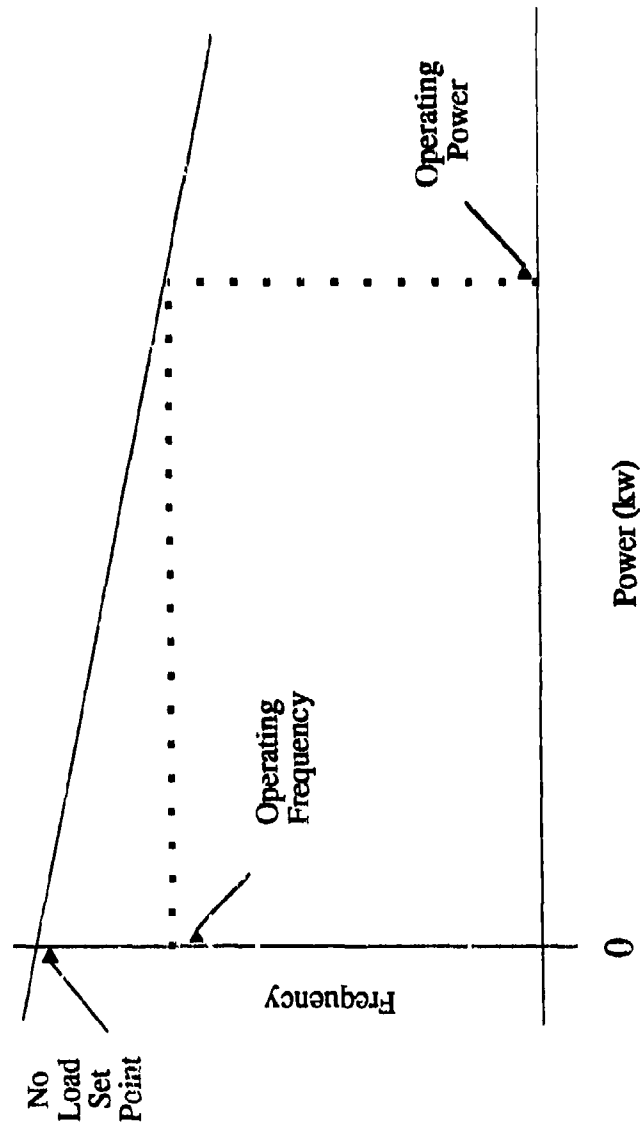
**Figure 4. House Diagram.**

22

function format of the plant, speed block, and speed regulator is then reduced to a single open loop to study the roots of the system as the regulator gain $K$ is varied. This complete process is demonstrated in Figures 5, 5a, 5b, and 5c. The resulting root locus plot is shown in Figure 6. The operating constraint was determined for the first root meeting the imaginary axis for a given $K$. The limit of $K$ was determined to be 153.
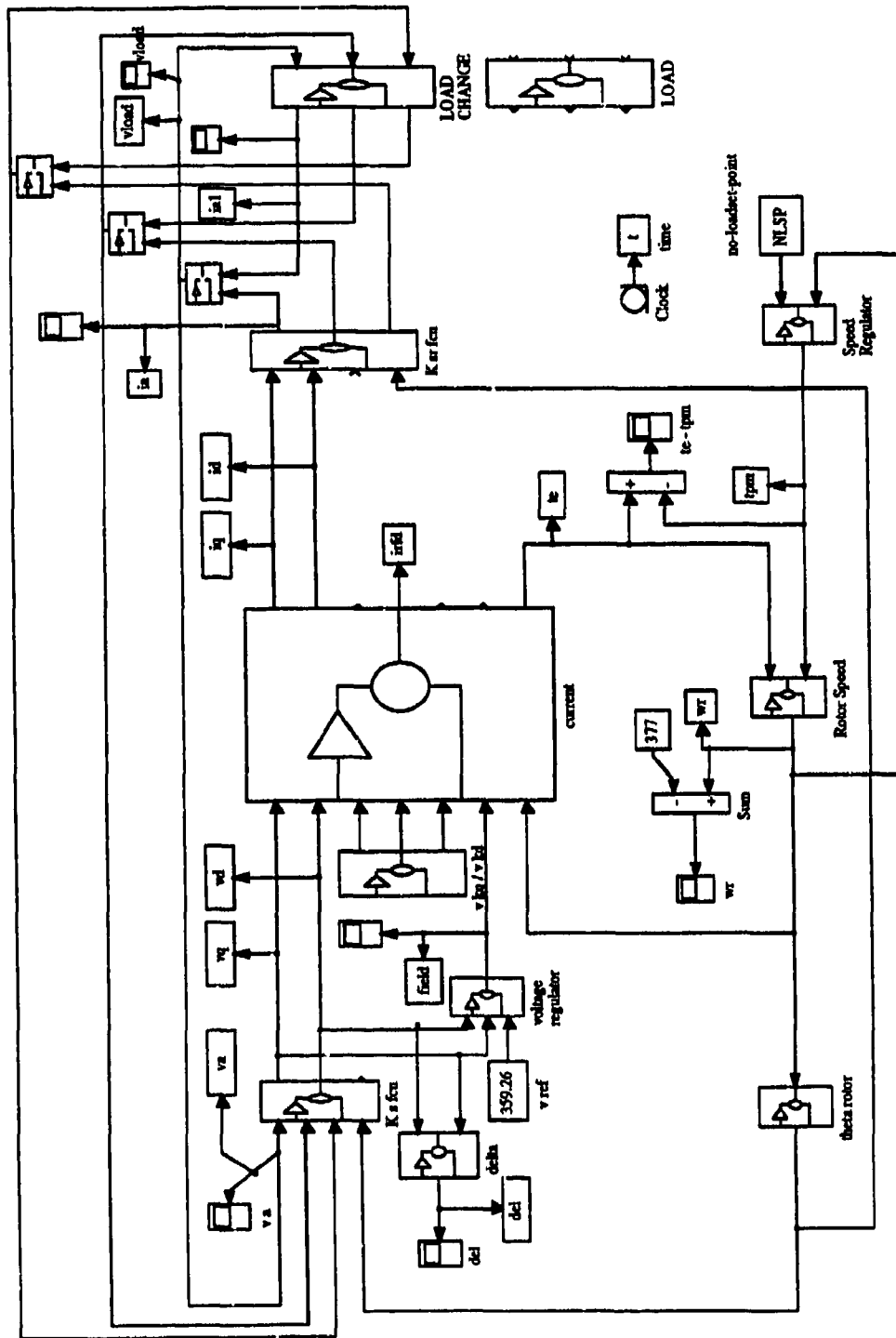
Figure 5. Synchronous Machine Model.

24

**Figure 5a. Current Block.**

25

**Figure 5b. Linearized Current Block, Speed Regulator, and Speed Block.**

26
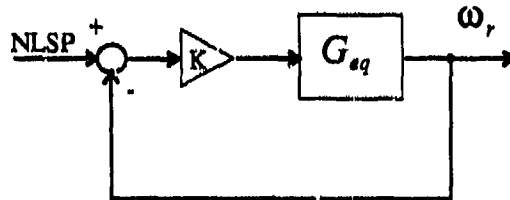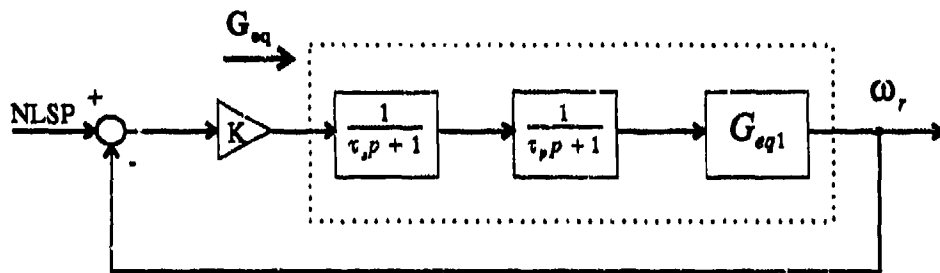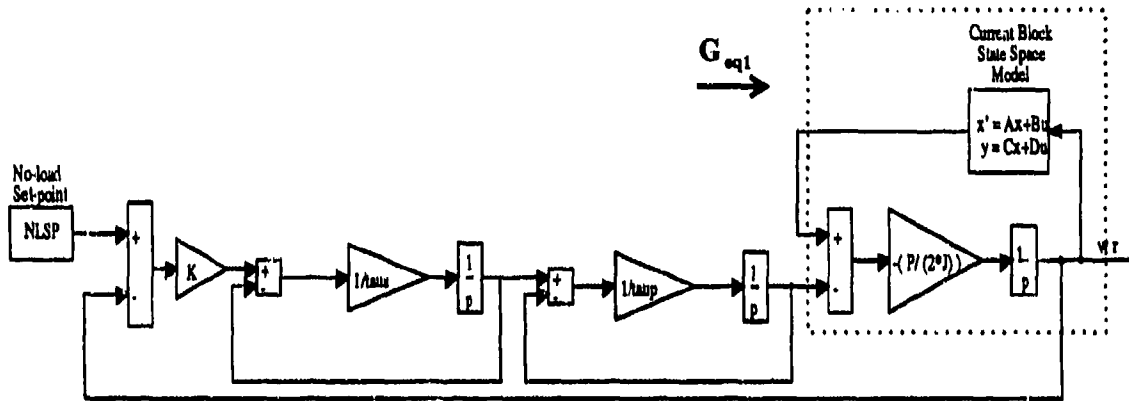
$$G_{cq1} = \frac{-K_2}{(p - K_2 \frac{num_{plant}}{den_{plant}})}$$

$$K_2 = \frac{P}{(2J)}$$

$$G_{eq} = conv\left[\left(\frac{1}{\tau_s p + 1}\right)\left(\frac{1}{\tau_p p + 1}\right)(G_{eq1})\right]$$

**Figure 5c.  Transfer Function Development, Speed Regulator.**

27
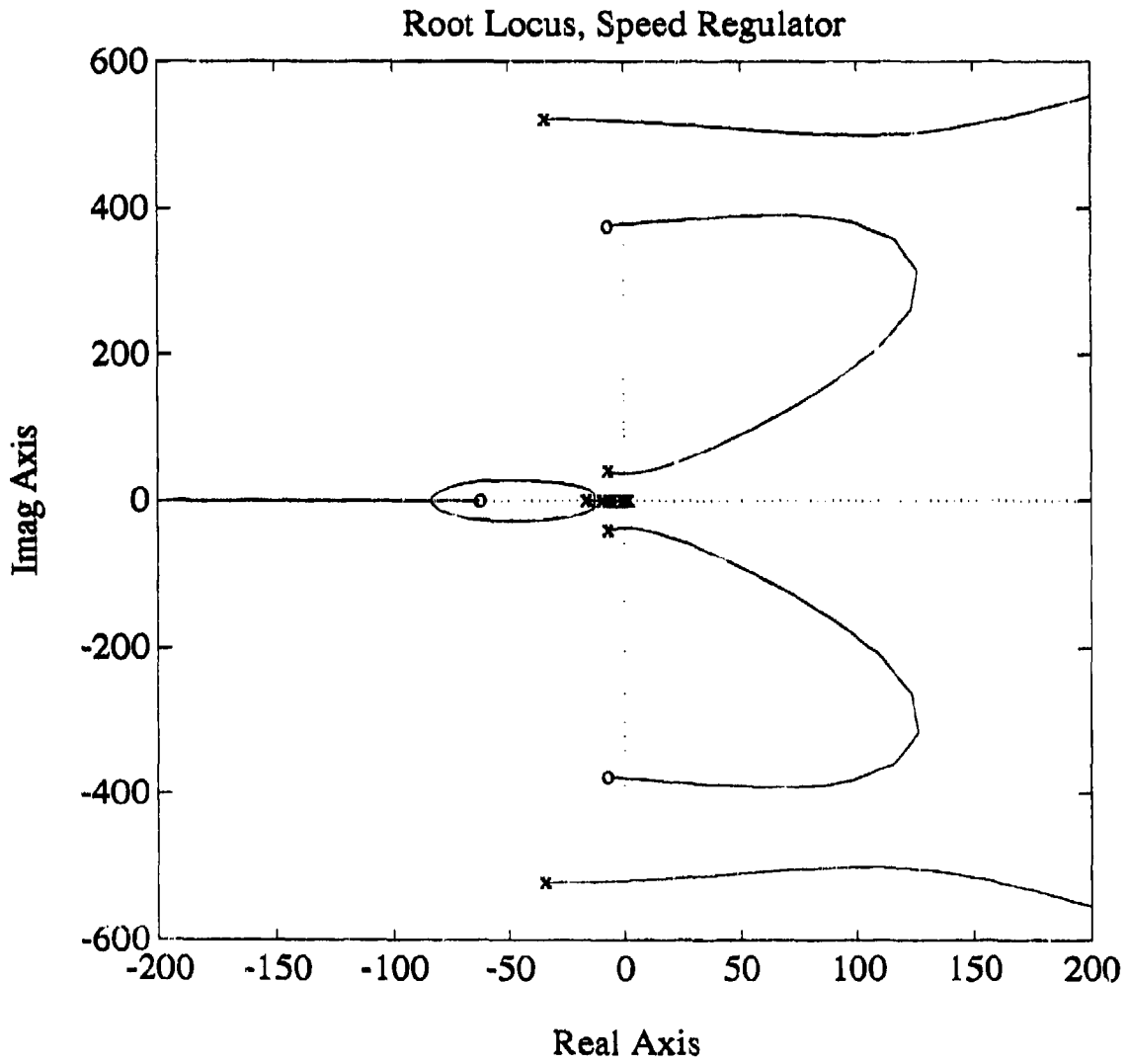
**Figure 6. Root Locus Plot--Synchronous Machine and Speed Regulator.**

28

## B. VOLTAGE REGULATOR

The voltage regulator or excitation system used in this study is shown in block diagram form in Figure 7 [6]. The parameters are defined as follows

$\tau_A$ and $K_A$          Regulator amplifier gain and time constant

$\tau_E$ and $K_E$          Saturating exciter gain and time constant

$\tau_{F1}$ , $\tau_{F2}$ , and $K_F$      Feedback loop gain and time constants

The SIMULINK model developed from the block diagram is shown in Figure 8. The regulator compares the bus voltage with the specified reference voltage. As can be seen in the Simulink model, this comparison is done in the $qd0$ reference frame.

The reference voltage is computed as follows

$$v_{reference} = \sqrt{\overline{v_q}^2 + \overline{v_d}^2} \tag{63}$$

This equates to the desired line-to-neutral voltage (peak) as shown below

$$\mathbf{v}_{qd0s} = \frac{2}{3}\mathbf{K}_s'\mathbf{v}_{abcs} \tag{64}$$

$$\begin{bmatrix} v_q \\ v_d \\ v_0 \end{bmatrix} = \frac{2}{3} \begin{bmatrix} \cos\theta_r & \cos(\theta_r - \frac{2\pi}{3}) & \cos(\theta_r + \frac{2\pi}{3}) \\ \sin\theta_r & \sin(\theta_r - \frac{2\pi}{3}) & \sin(\theta_r + \frac{2\pi}{3}) \\ \frac{1}{2} & \frac{1}{2} & \frac{1}{2} \end{bmatrix} \begin{bmatrix} v_a \\ v_b \\ v_c \end{bmatrix} \tag{65}$$

29
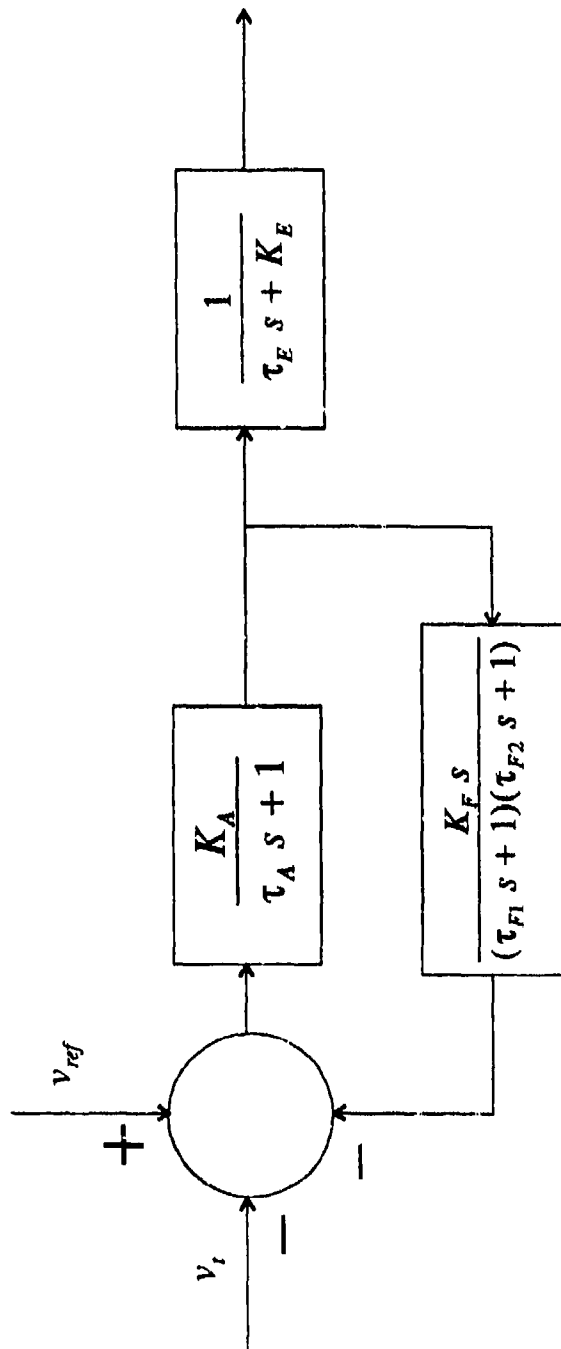
**Figure 7. Block Diagram, Voltage Regulator.**

30
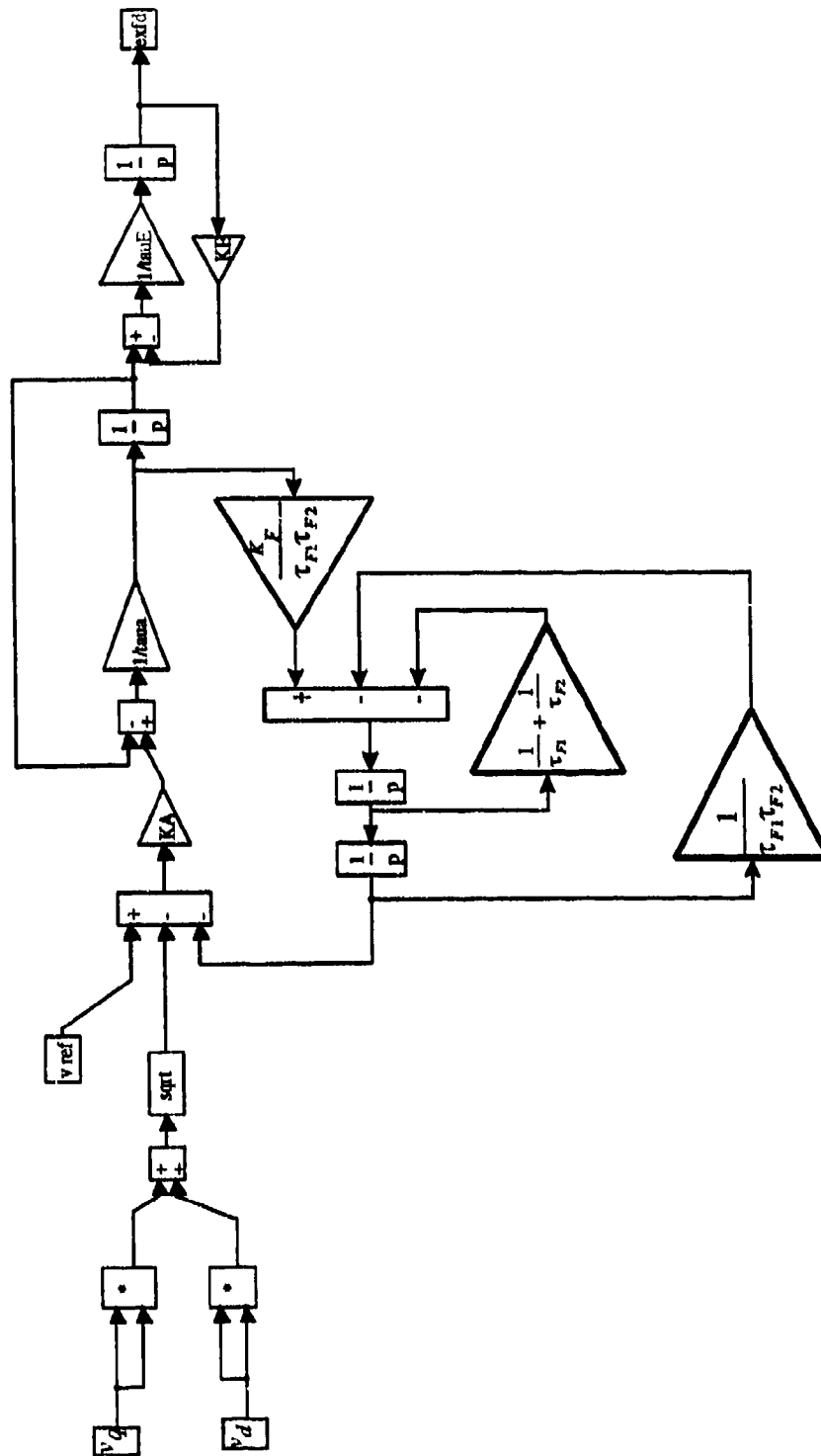
**Figure 8. SIMULINK Voltage Regulator.**

31

where

$$v_a = v_{ln}\cos(\theta_{ev})$$

$$v_b = v_{ln}\cos(\theta_{ev} - \frac{2\pi}{3})$$

$$v_c = v_{ln}\cos(\theta_{ev} + \frac{2\pi}{3})$$

(66)

and

$$\theta_r = \int_0^t \omega_r(\xi)\, \xi d + \theta_r(0)$$

$$\theta_{ev} = \int_0^t \omega_e(\xi)\, \xi d + \theta_{ev}(0)$$

(67)

and solving for $v_q$ and $v_d$

$$v_q = \frac{2}{3}v_{ln}\left[\cos\theta_r\cos\theta_{ev} + \cos(\theta_r - \frac{2\pi}{3})\cos(\theta_{ev} - \frac{2\pi}{3}) + \cos(\theta_r + \frac{2\pi}{3})\cos(\theta_{ev} + \frac{2\pi}{3})\right]$$

(68)

$$v_d = \frac{2}{3}v_{ln}\left[\sin\theta_r\cos\theta_{ev} + \sin(\theta_r - \frac{2\pi}{3})\cos(\theta_{ev} - \frac{2\pi}{3}) + \sin(\theta_r + \frac{2\pi}{3})\cos(\theta_{ev} + \frac{2\pi}{3})\right]$$

(69)

and using the trigonometric identities

$$\cos x\cos y + \cos(x - \frac{2\pi}{3})\cos(y - \frac{2\pi}{3}) + \cos(x + \frac{2\pi}{3})\cos(y + \frac{2\pi}{3}) = \frac{3}{2}\cos(x - y)$$

(70)

$$\sin x\cos y + \sin(x - \frac{2\pi}{3})\cos(y - \frac{2\pi}{3}) + \sin(x + \frac{2\pi}{3})\cos(y + \frac{2\pi}{3}) = \frac{3}{2}\sin(x - y)$$

(71)

32

gives

$$v_q = \frac{2}{3} v_{ln} \frac{3}{2} \cos(\theta_r - \theta_{ev}) \tag{72}$$

$$= v_{ln} \cos[(\omega_r - \omega_e)t + \theta_r(0) - \theta_{ev}(0)]$$

$$v_d = \frac{2}{3} v_{ln} \frac{3}{2} \sin(\theta_r - \theta_{ev}) \tag{73}$$

$$= v_{ln} \sin[(\omega_r - \omega_e)t + \theta_r(0) - \theta_{ev}(0)]$$

At synchronous speed $\omega_r = \omega_e$, and from (61) $\delta \approx \theta_r - \theta_{ev}$, therefore

$$v_q = v_{ln} \cos(\delta) \tag{74}$$

$$v_d = v_{ln} \sin(\delta) \tag{75}$$

and

$$v_{reference} = \sqrt{v_{ln}^2 [\cos^2(\delta) + \sin^2(\delta)]} = v_{ln} \tag{76}$$

# III.   MACHINE LOAD

To accurately study the machine's performance it is necessary to be able to load the given machine in a realistic manner. The inductive nature of transmission lines and induction motors dictate a need for a resistive-inductive (RL) loading of the machine.

This section develops the RL-load used for the synchronous generator and then the SIMULINK implementation of this loading.

## A.   PASSIVE RL-LOAD

The load used for this study was comprised of a passive resistive-inductive load. This loading is typical of ac motors, transmission lines, electric heating, and lighting. The load was modeled in $abc$-variables in order to eliminate the need for additional transformations ($abc \rightarrow qd0$). The simulation uses voltage as the input and currents as the outputs. This requires the phase voltages to be made up from the network equations. The loads also use voltage as the inputs and current as the outputs. Based on this topology it is advantageous to assume a Y-connected set of large resistors are connected across the terminals of the synchronous generator [7] and the phase voltages at the terminals of the generator are computed from

$$v_a = - R(i_{aG} + i_{aL}) \tag{85}$$

$$v_b = - R(i_{bG} + i_{bL}) \tag{86}$$

$$v_c = - R(i_{cG} + i_{cL}) \tag{87}$$

where $i_{aG}$, $i_{bG}$, and $i_{cG}$ are the phase currents flowing into the generator from the load and $i_{aL}$, $i_{bL}$, and $i_{cL}$ are the phase currents flowing into the load from the generator. These

34

currents are computed first as $i_q$, $i_d$, and $i_0$ and then transformed to $i_a$, $i_b$, and $i_c$. This is represented in Figure 9.

This load modeling is quite accurate as the resistance value $R$ is made large (20-50 pu). As the resistance is made large, the current through this branch becomes negligible.

## B. SIMULINK LOAD MODEL

The passive $RL$-load was modeled in SIMULINK by starting with the voltage equations (only developed for phase a, others similar) from Figure 10.

$$v_a = e_a + L_s p i_a + r_s i_a \tag{88}$$

$$v_a = r_L + L_L p i_L \tag{89}$$

$$v_a = R(i_a - i_L) \tag{90}$$

The differential equations can be implemented as shown in Figure 11.

As can be seen, the terminal voltage $v_a$ is dependent on the output current $i_a$. This voltage dependency is the difference between a finite and an infinite bus model of electric machines. An infinite bus analysis assumes no dependency between $v_a$ and $i_a$.

An attempt was made to make the load purely resistive. SIMULINK is unable to deal with this type of load however since this would incorporate direct feed-through between input and output of the load. This forms an algebraic loop and cannot be analyzed. The inductance of the transmission line overcomes this limitation. The purely resisitve load, connected by a transmission line (with inherent inductance) to the generator bus adds sufficient inductance to warrant modeling. This inductance then incorporates a time-delay between input and output due to the integral form of the load equations.
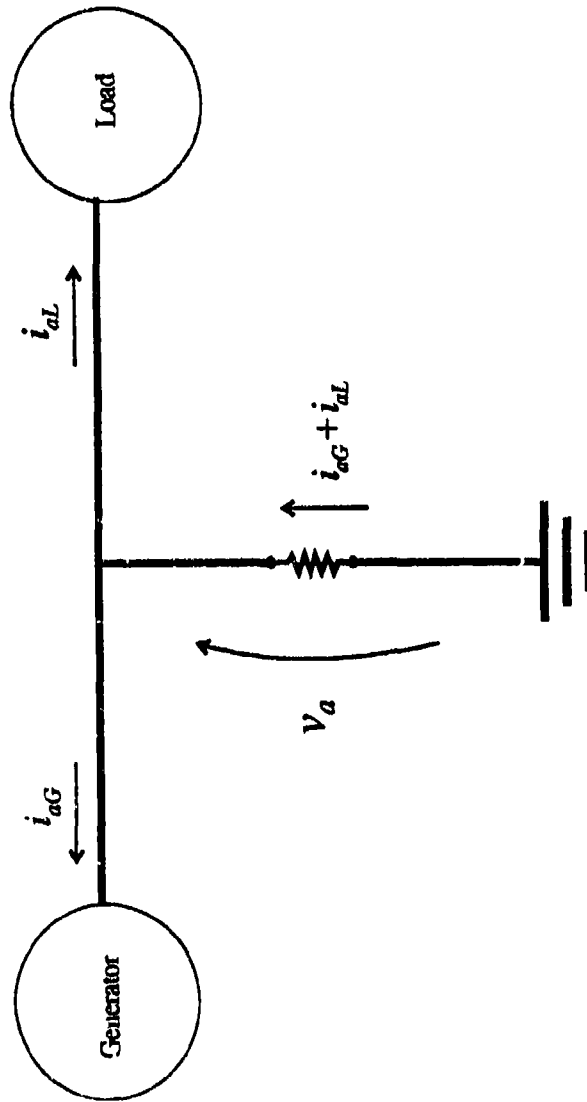
Figure 9. Generator Terminal Voltage Model.
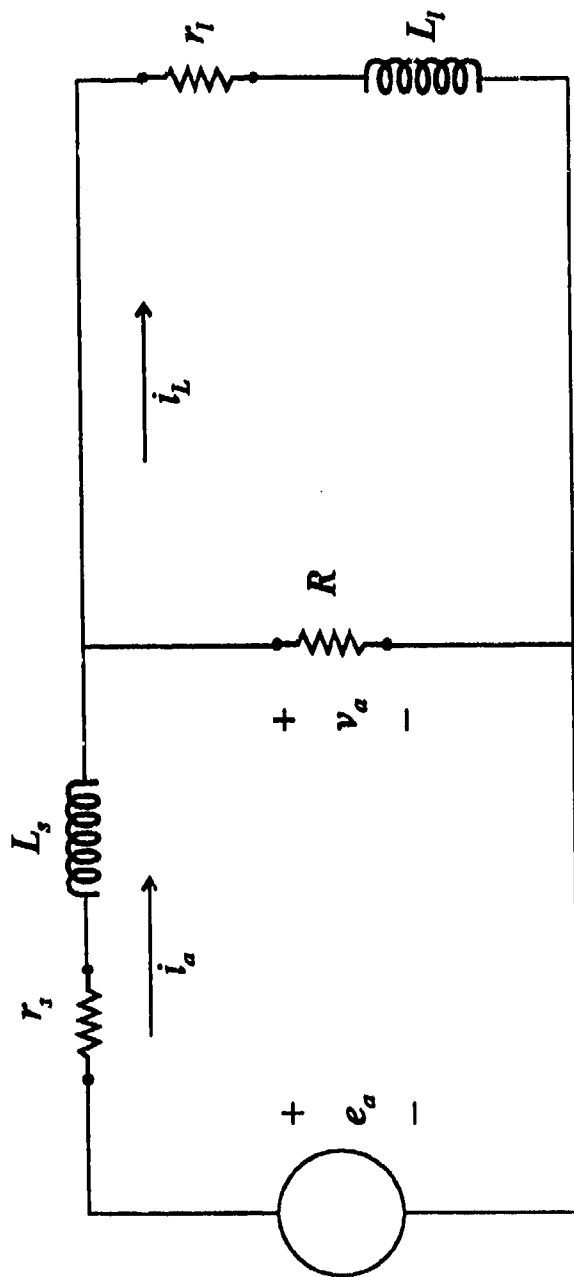
Figure 10. Passive RL-Load Model.
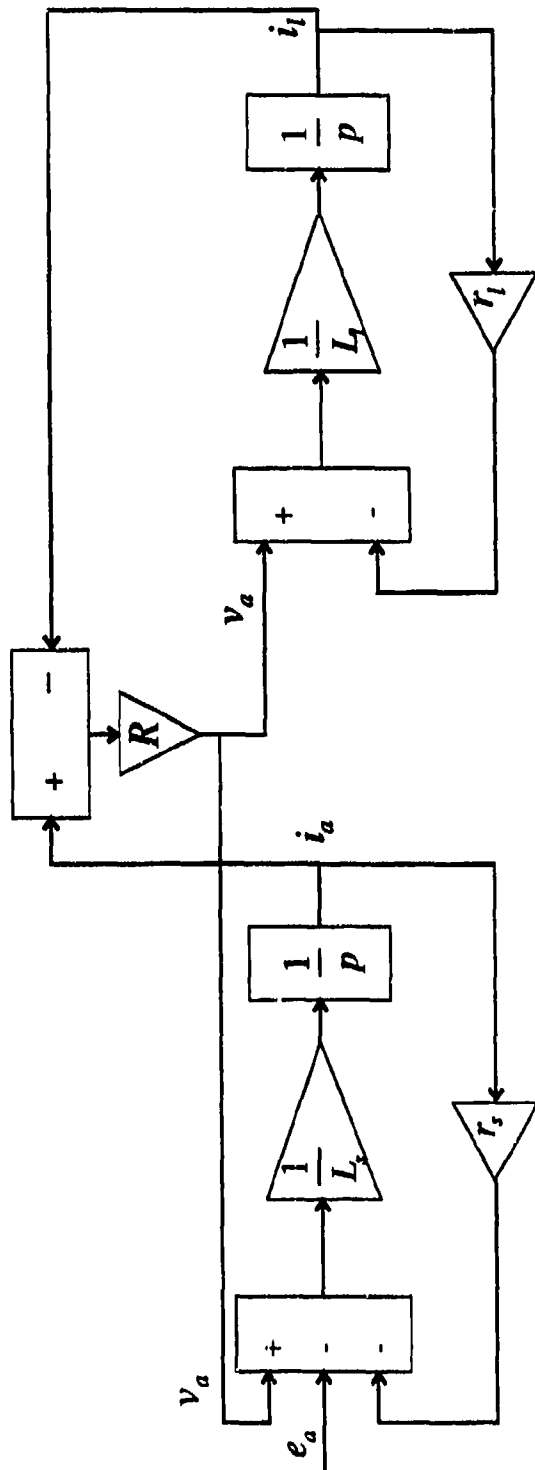
Figure 11. Differential Equation Implementation of Voltage Equations.

# IV.  MACHINE MODEL PERFORMANCE

The synchronous machines performance is examined in this section. The machines parameters are given and the machines response to both a load change and a fault condition are studied.

## A.  MACHINE PARAMETERS

The machine being simulated is a 4-pole, 60 Hz, 440 V (line-to-line), 500 kW, 0.85 power factor synchronous generator. The per unit parameters on the machine base ($Z_{base}$ = 0.1291 $\Omega$) are as follows

stator resistance, $r_s$ = 0.00031

rotor field resistance, $r_{fd}$ = 0.00226

q-axis damper winding resistance, $r_{kq}$ = 0.0224

d-axis damper winding resistance, $r_{kd}$ = 0.00673

stator leakage reactance, $X_{ls}$ = 0.0632

d-axis magnetizing reactance, $X_{md}$ = 1.4648

q-axis magnetizing reactance, $X_{mq}$ = 0.7668

field leakage reactance, $X_{lfd}$ = 0.1545

q-axis damper winding leakage reactance, $X_{lkq}$ = 0.0771

d-axis damper winding leakage reactance, $X_{lkd}$ = 0.3676

rotor inertia, $J$ = 14.526

These machine parameters are taken from the Machinery Systems Laboratory (MSL) test facility for a typical shipboard synchronous generator [8]. The MSL test facility is within

the Machinery Systems Engineering Branch at David Taylor Naval Ship Research and Development Center.

## B.  SIMULATION: LOAD CHANGE

The machine was initially loaded at an approximate power factor of 0.8, with the load calculated as follows

Machine data:    440-V   1.5 MVA.  From Figure 12

$$\left|\tilde{I}\right| = \frac{1.5e6}{3}\frac{1}{254} = 1.969\ kA \tag{91}$$

$$\tilde{I} = 1.969\ e^{-j\cos^{-1}(0.8)}\ kA \tag{92}$$

$$\tilde{Z} = \frac{254\ e^{j0}}{1.969\,e^{-j36.87^{\circ}}kA} = 129\ e^{j36.87^{\circ}}\ m\Omega \tag{93}$$

$$r_L = 103.2\ m\Omega \qquad X_L = 77.42\ m\Omega \tag{94}$$

With the machine loaded as above, the expected steady-state power delivered to the load will be approximately 1.2 MW. This does not however account for the losses in the stator windings.   The machine then underwent a 50 % step load change by doubling the values of $r_L$ and $X_L$ .  This was done in SIMULINK by the load-change block shown in Figure 13. The plots of the response are shown in Figures 14 through 21. The data obtained from the simulation was as follows:

|  | FULLY LOADED MODEL | 50% LOADED MODEL |
|---|---|---|
| Load power, MW | 1.1754 | 0.5186 |
| Machine power, MW | 1.1792 | 0.5151 |
| Frequency, Hz | 59.99 | 64.32 |
| Power Factor | 0.7992 | 0.7832 |

40
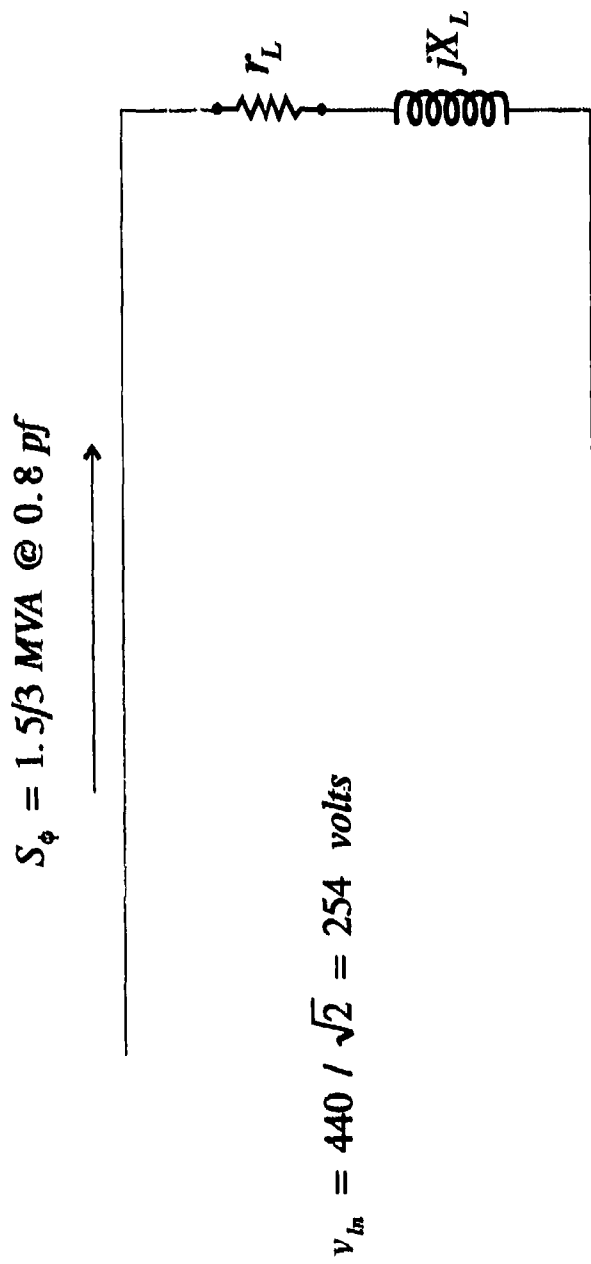
Figure 12. Initial Load Parameter Determination Circuit.
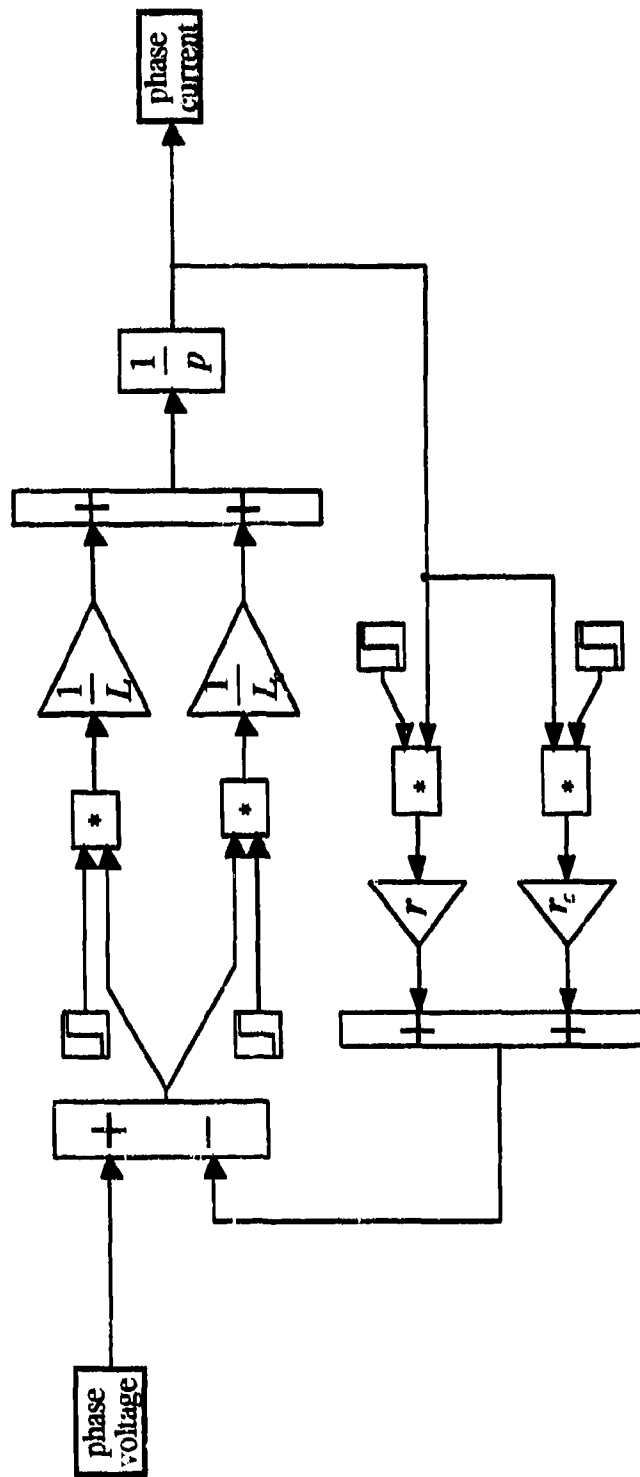
Figure 13. SIMULINK Load Change Block.

42
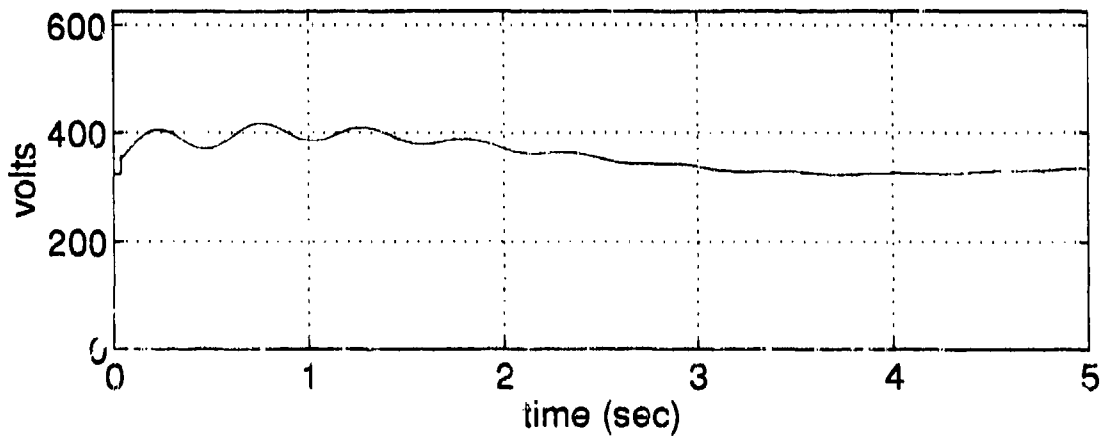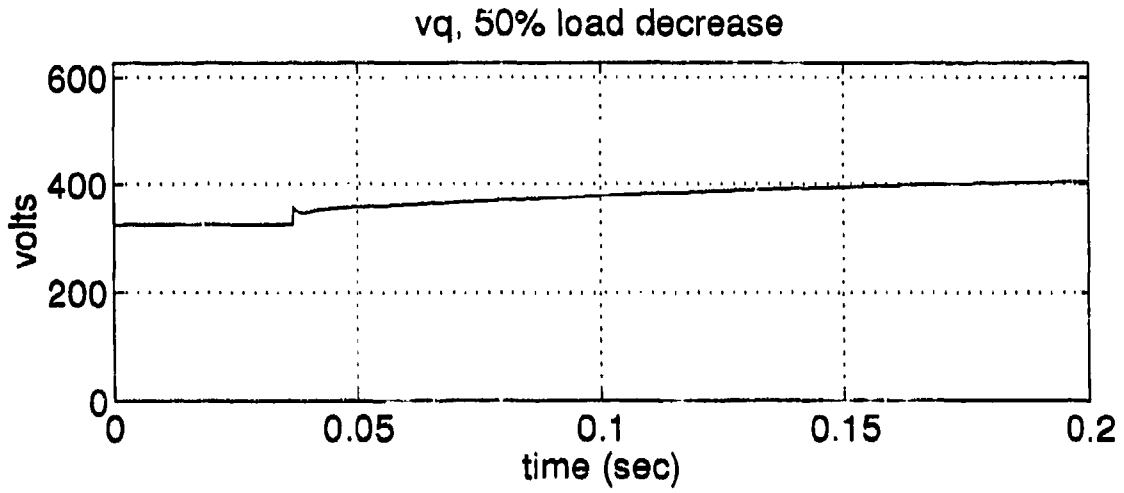
**Figure 14. 50 Percent Load Decrease, *vq*.**

43
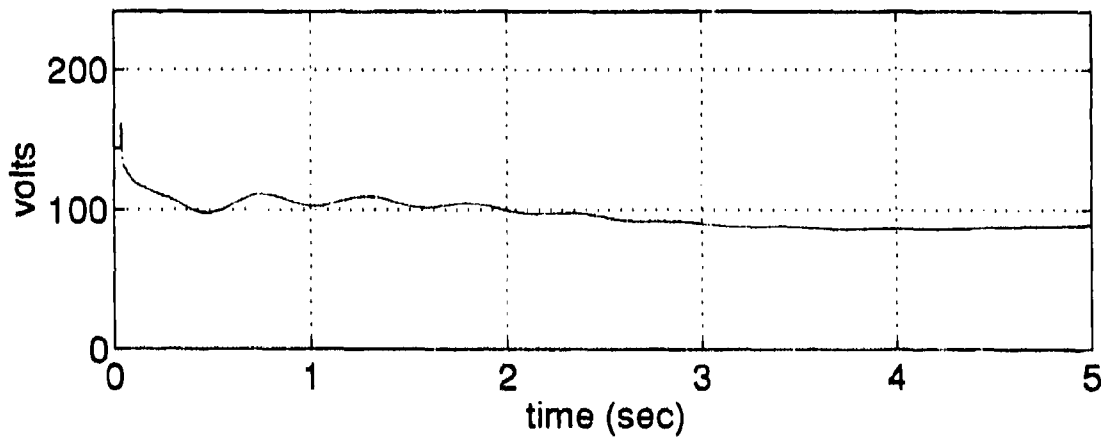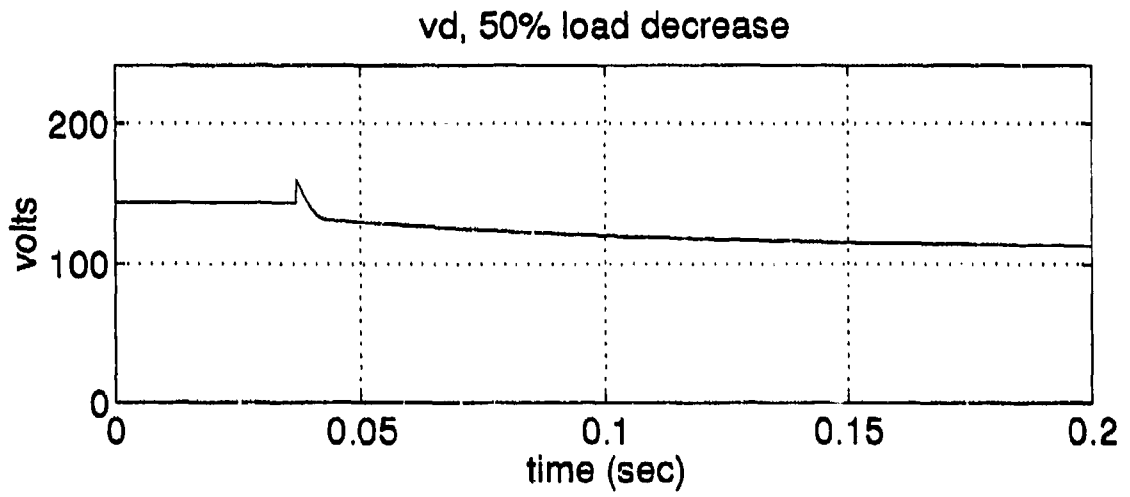
Figure 15. 50 Percent Load Decrease, *vd*.

44
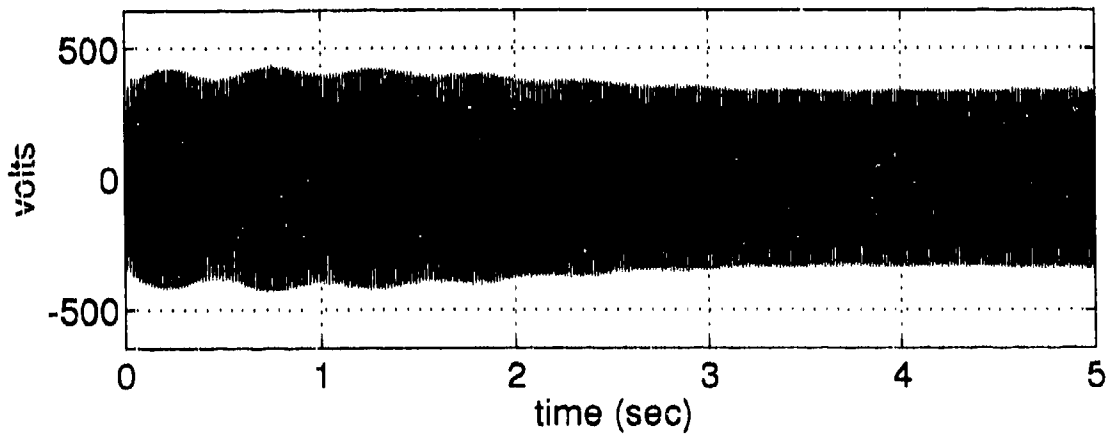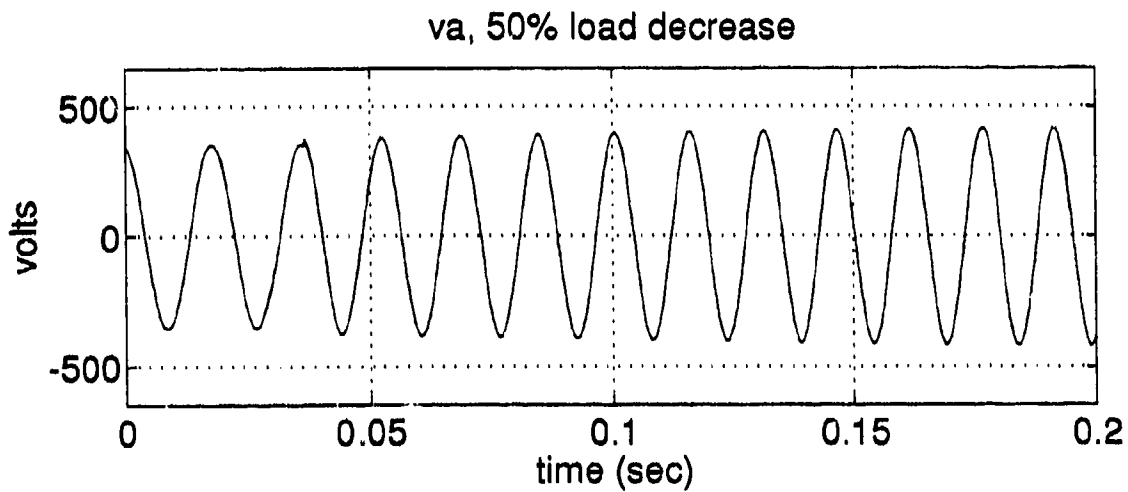
Figure 16. 50 Percent Load Decrease, *va*.
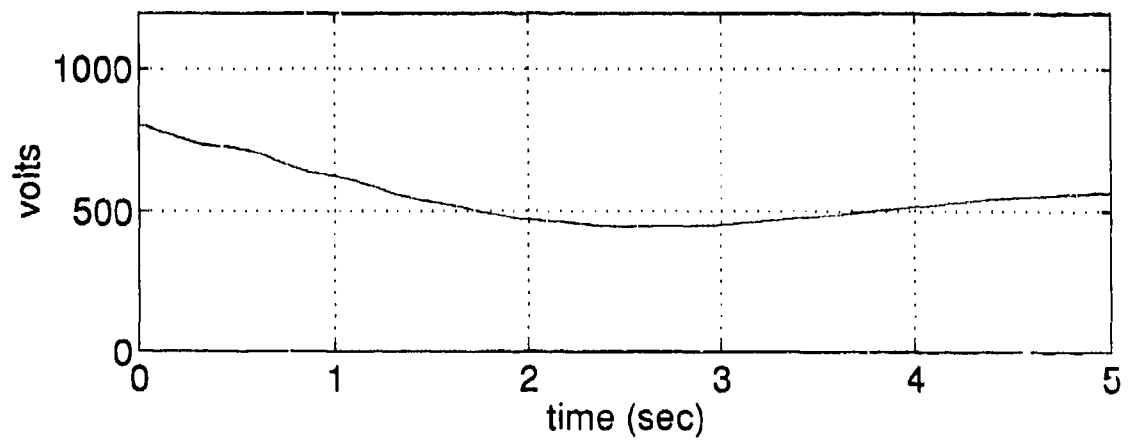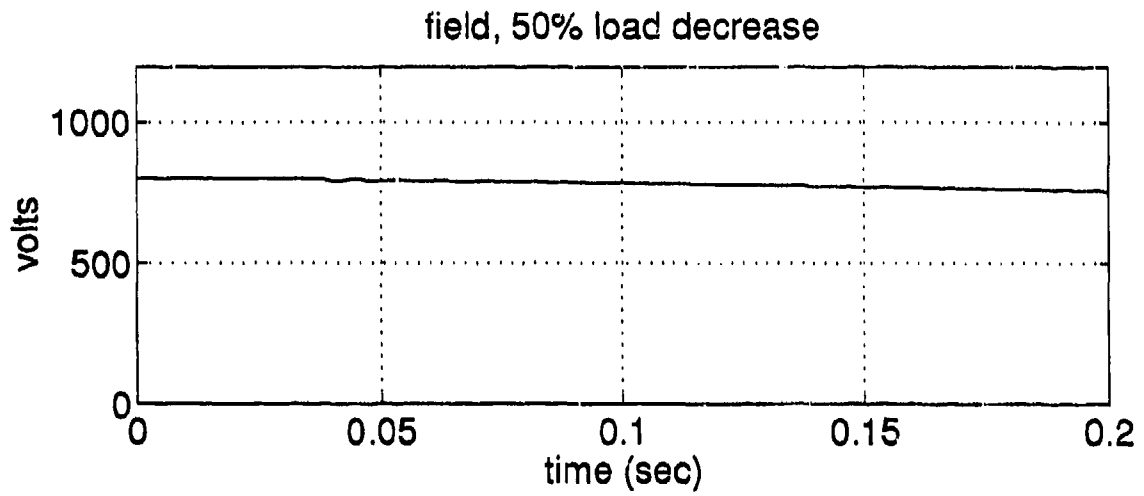
Figure 17. 50 Percent Load Decrease, *field voltage*.

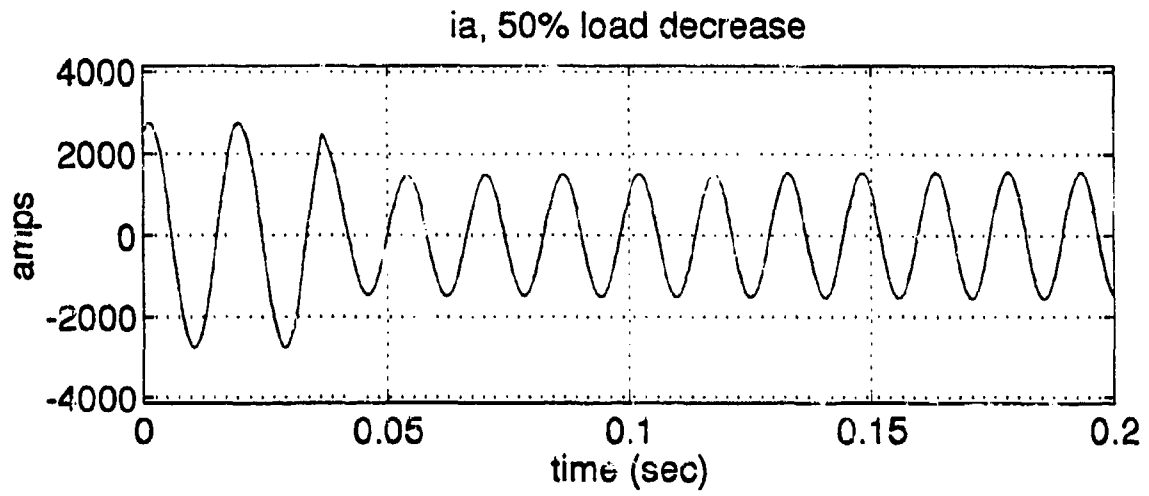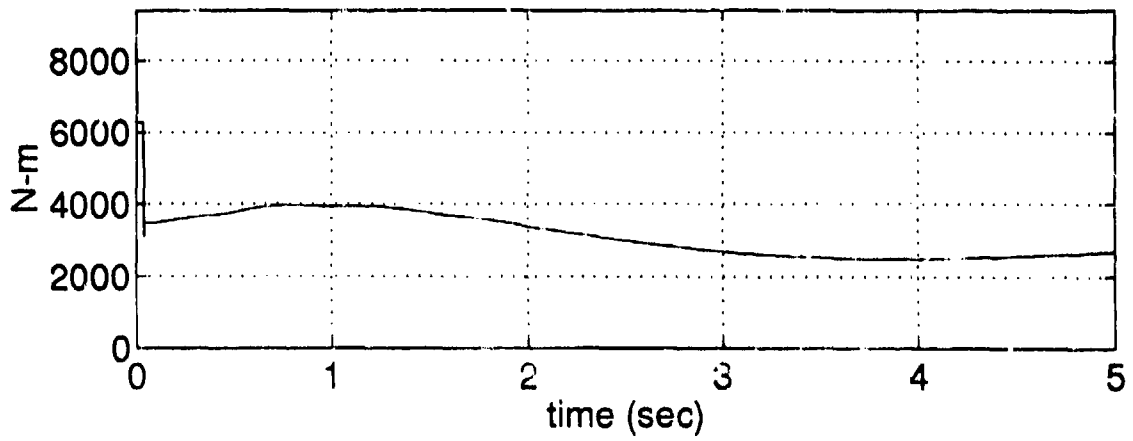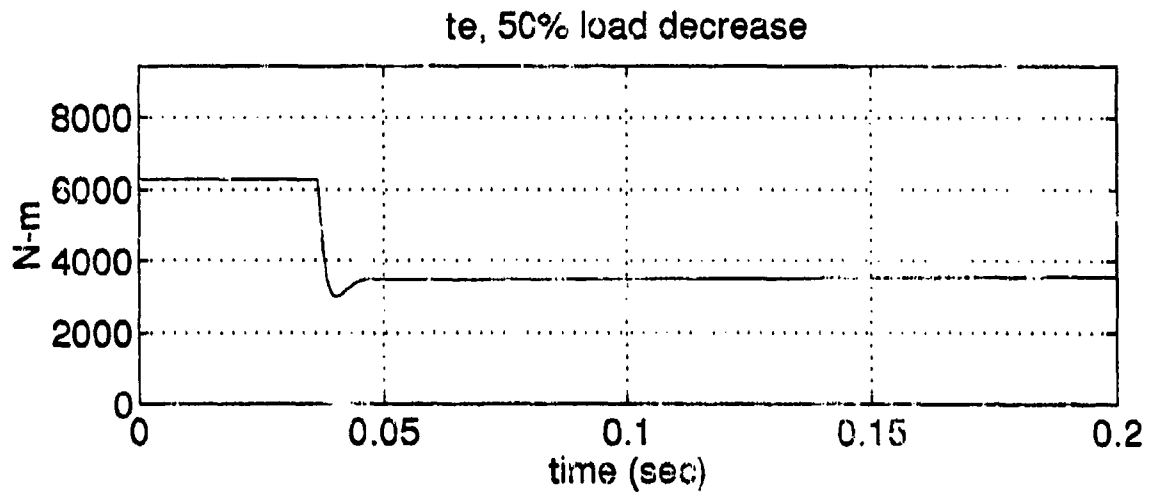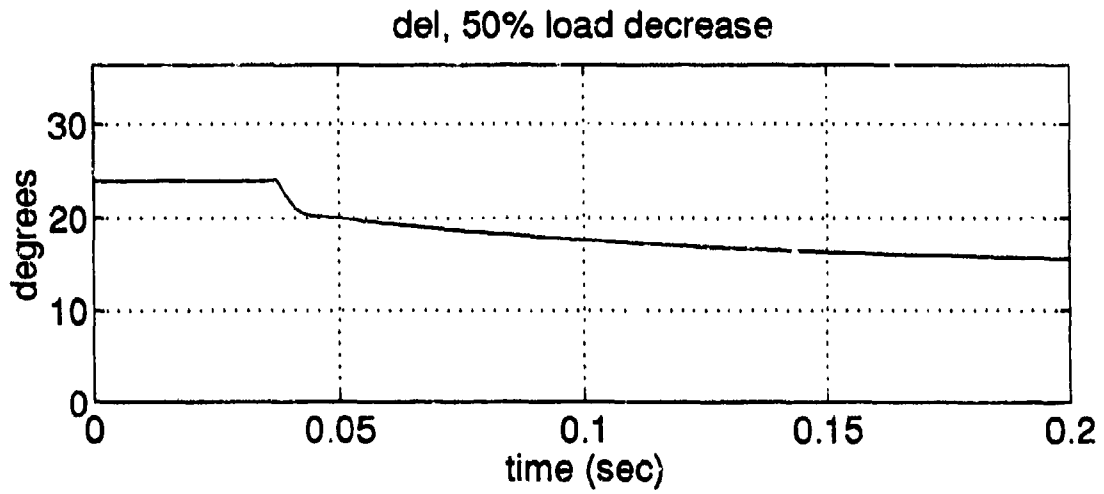46
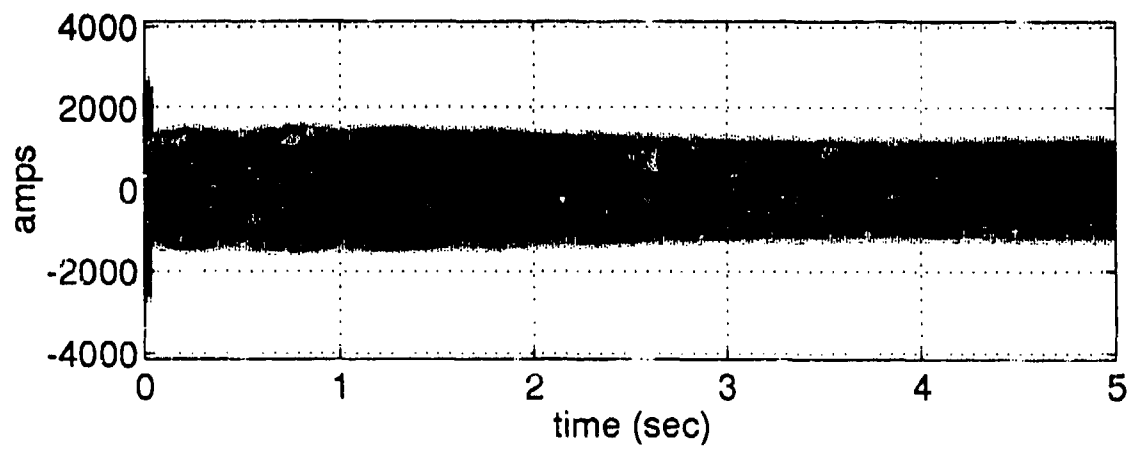
Figure 18. 50 Percent Load Decrease, *ia*.

te, 50% load decrease



Figure 19. 50 Percent Load Decrease, *te*.

48
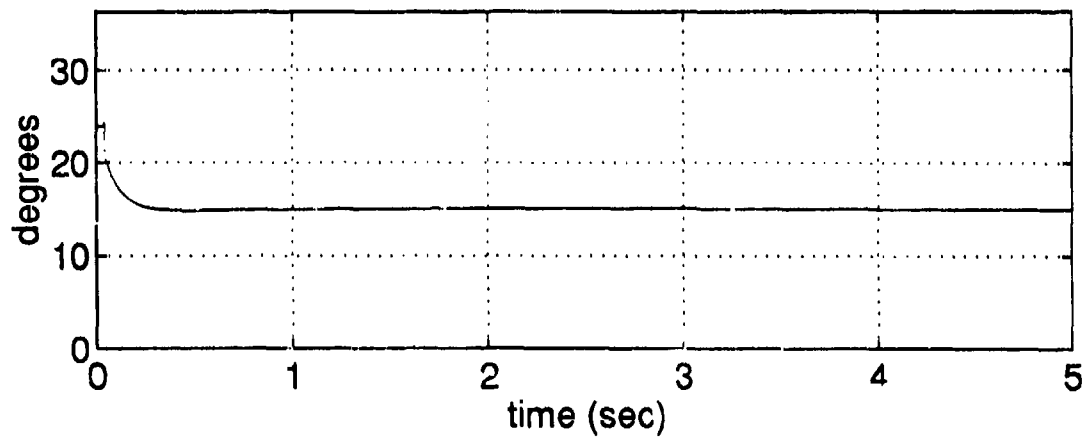
Figure 20. 50 Percent Load Decrease, *rotor angle (del)*.

49
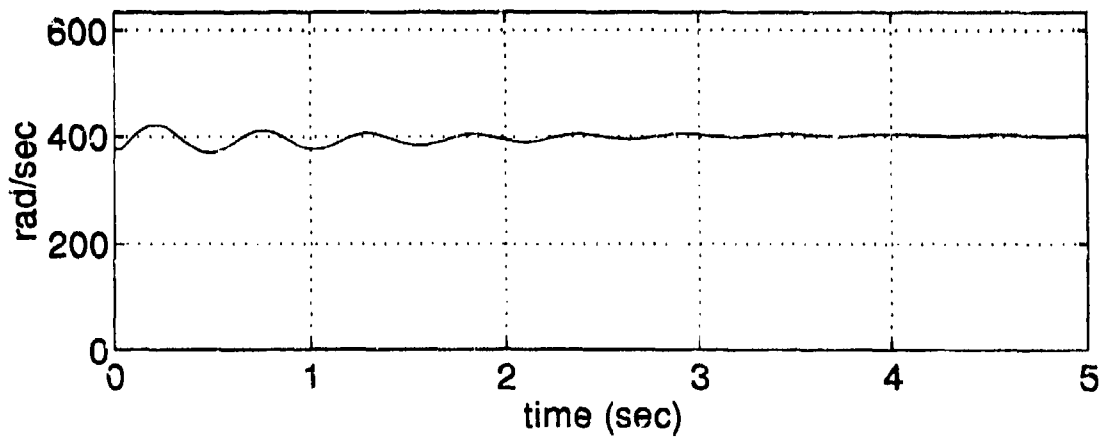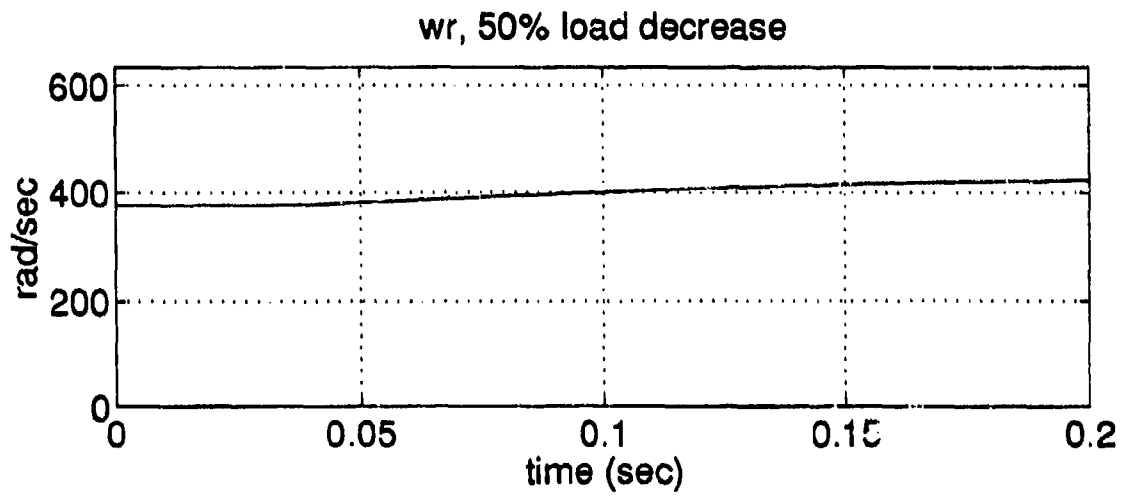
wr, 50% load decrease



Figure 21. 50 Percent Load Decrease, *rotor speed* ($\omega_r$).

## C. SIMULATION: THREE-PHASE FAULT

The stability of a synchronous machine throughout a power system following a fault is of major concern. A 3-phase fault or short-circuit rarely occurs and a 3-phase fault at the machine terminals is even more uncommon; however, it is still instructive to demonstrate the ability to insert a fault for a chosen time interval and study the machines dynamic performance.

The machine was initially loaded at a power factor of 0.8 as in part B. A 3-phase fault was inserted and was left in place for 7 cycles. The fault impedance (representative of the bus work) is $0.001291 + j\, 0.1291\ \Omega$. If the fault had been allowed to remain on the system slightly longer the machine would have become unstable in terms of not having returned to synchronous speed after removal of the fault or the machine would have slipped poles prior to returning to synchronous speed. It was determined that a seven-cycle fault is representative of a typical breaker reclosure timing cycle which the machine could have been subjected to.

The three-phase fault was performed in SIMULINK by the fault block shown in Figure 22. The fault implemented by using a step function block which stepped in the fault impedance at a particular time and then another step function block stepped in the normal load at the end of the desired fault time. The plots of the response are shown in Figures 23 through 30.
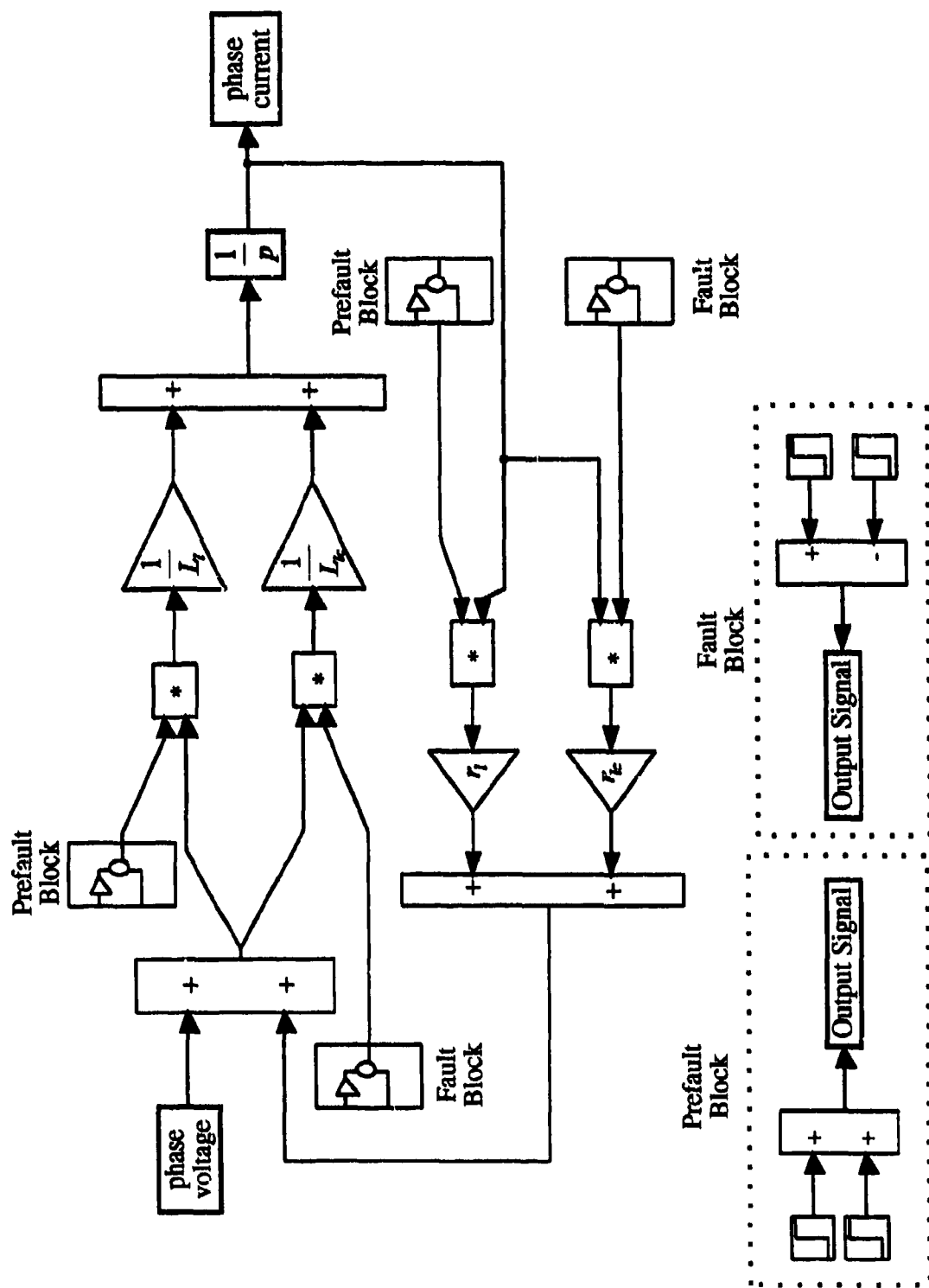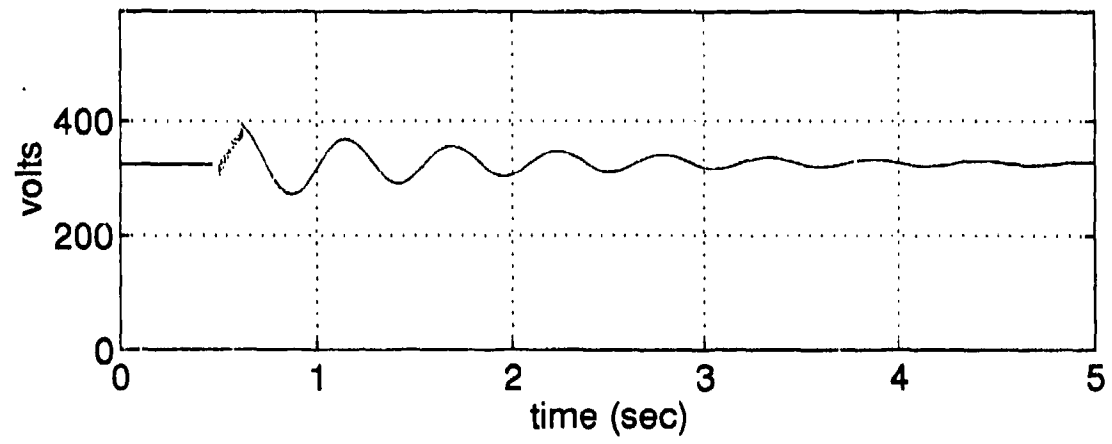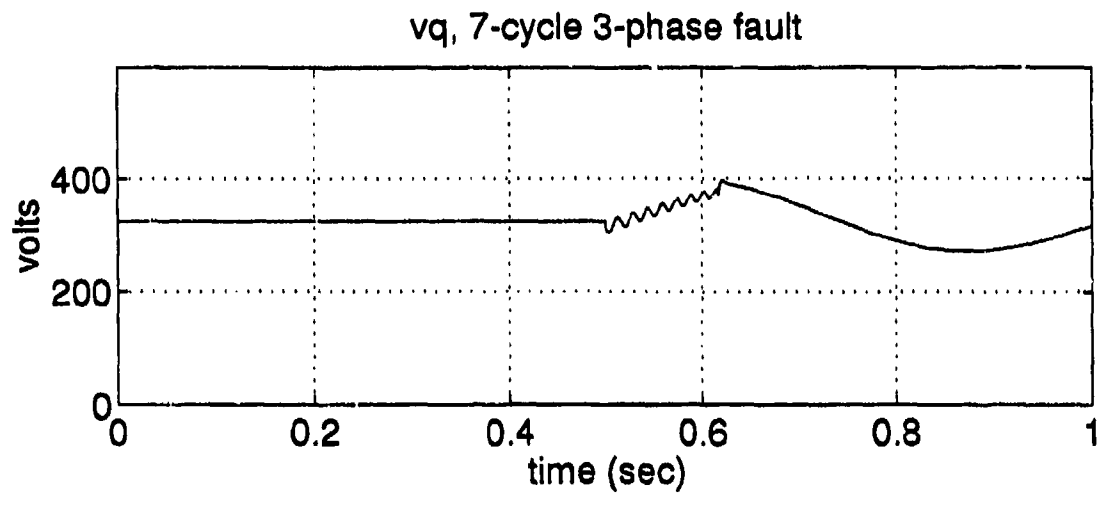
Figure 22. SIMULINK Three-Phase Fault Block.
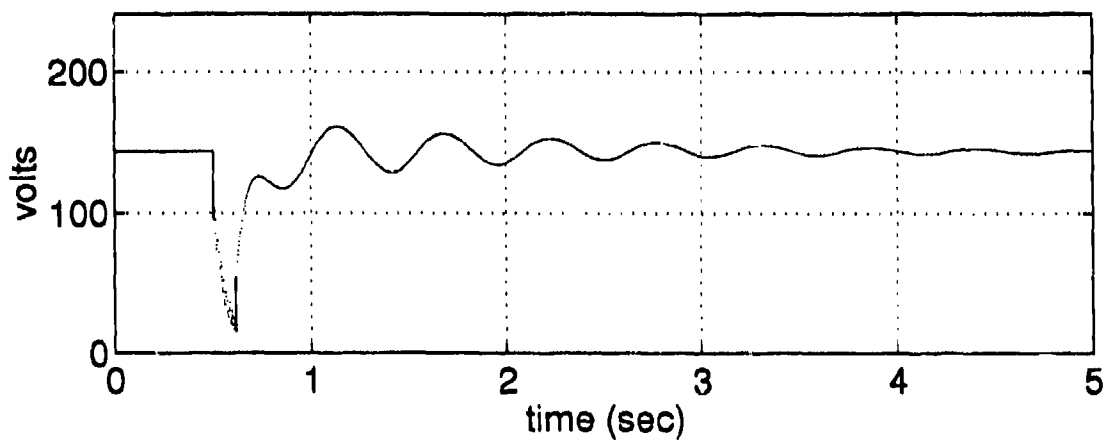
52

vq, 7-cycle 3-phase fault
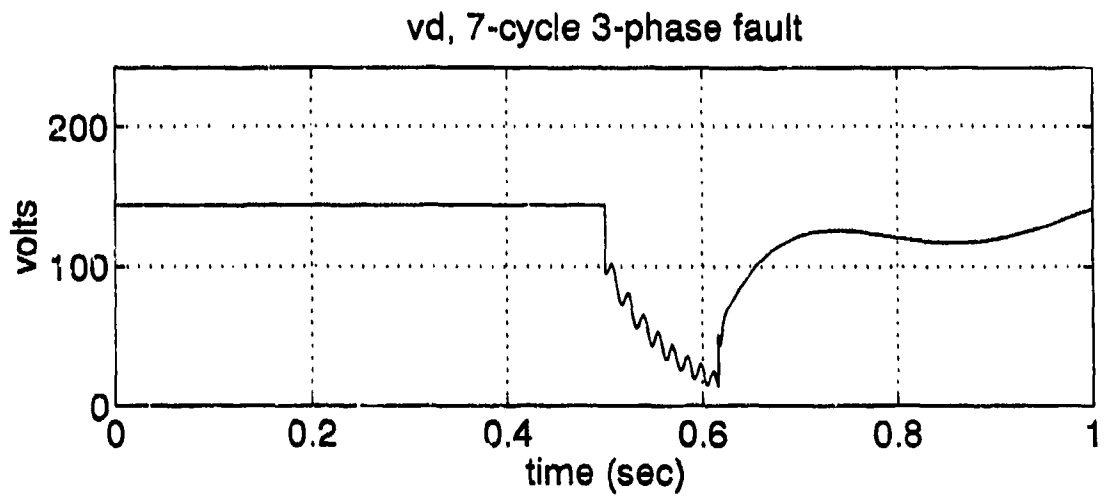


Figure 23. 7-Cycle, 3-Phase Fault, *vq*.

53

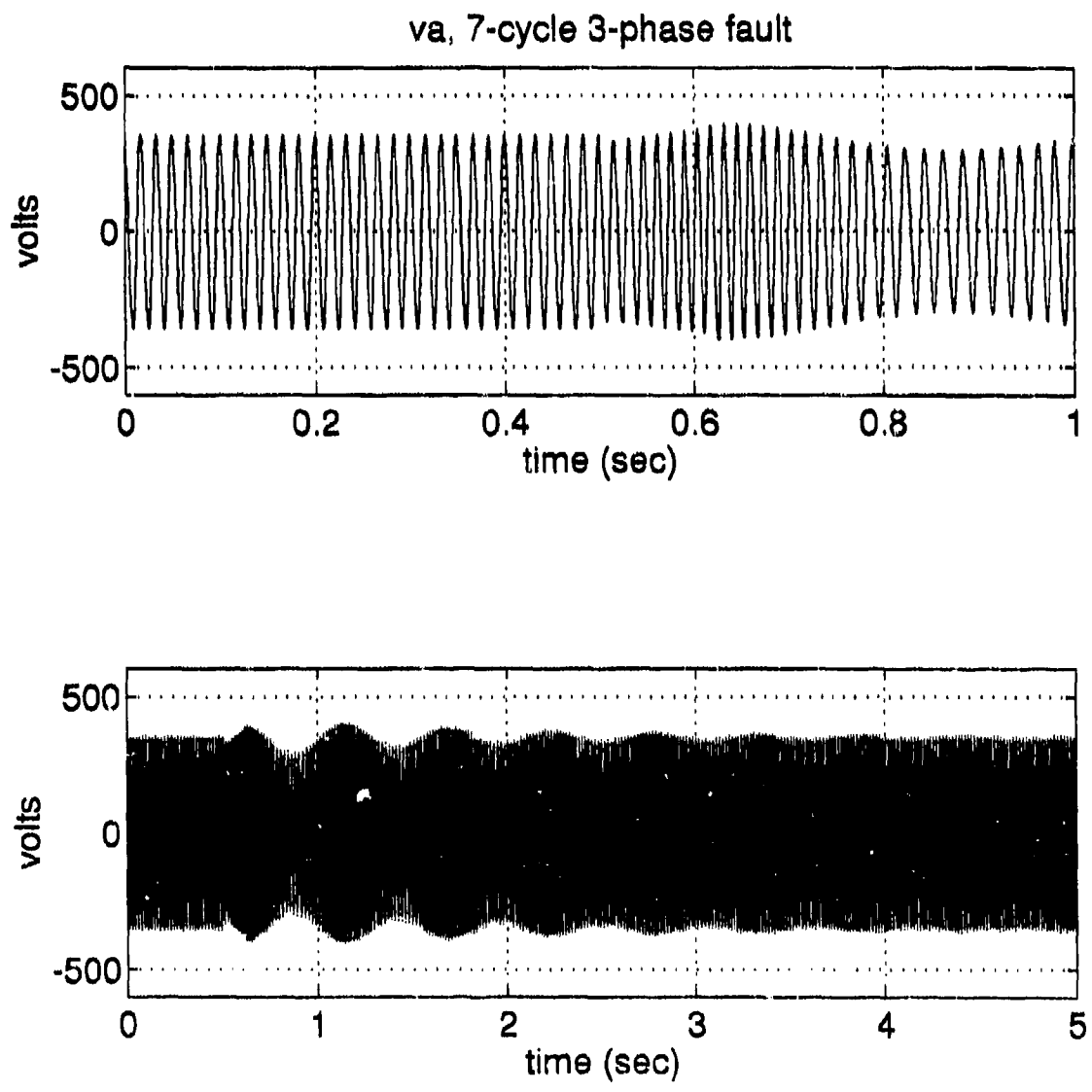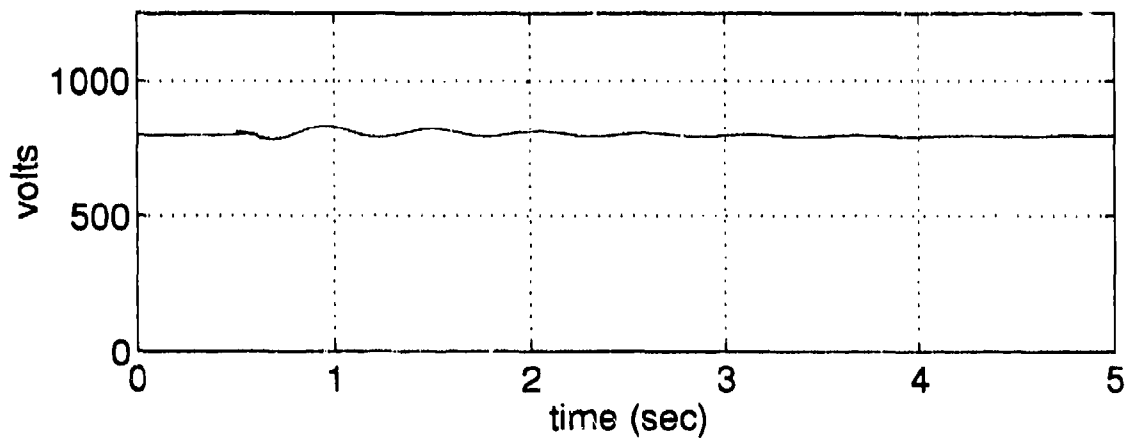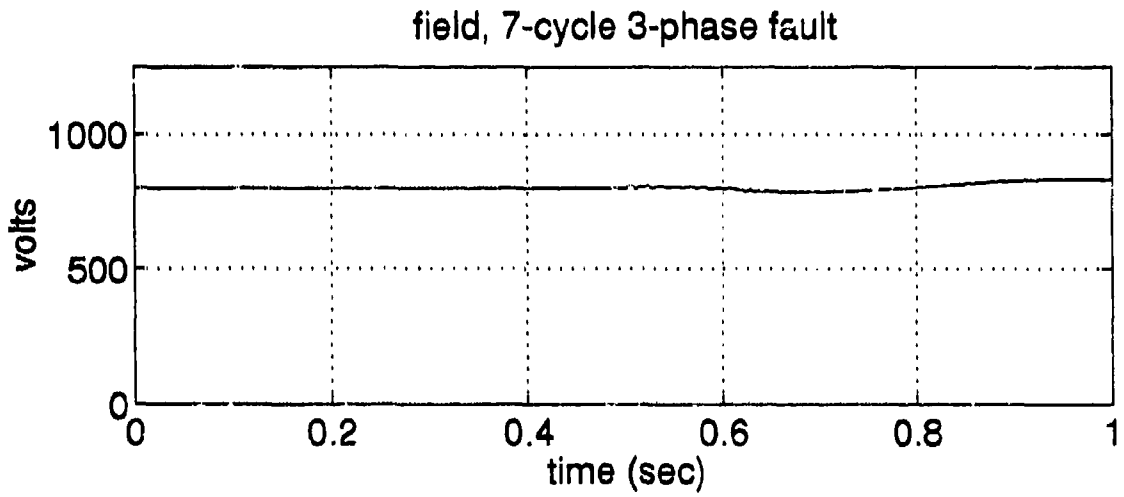**Figure 24. 7-Cycle, 3-Phase Fault, *vd*.**

Figure 25. 7-Cycle, 3-Phase Fault, *va*.
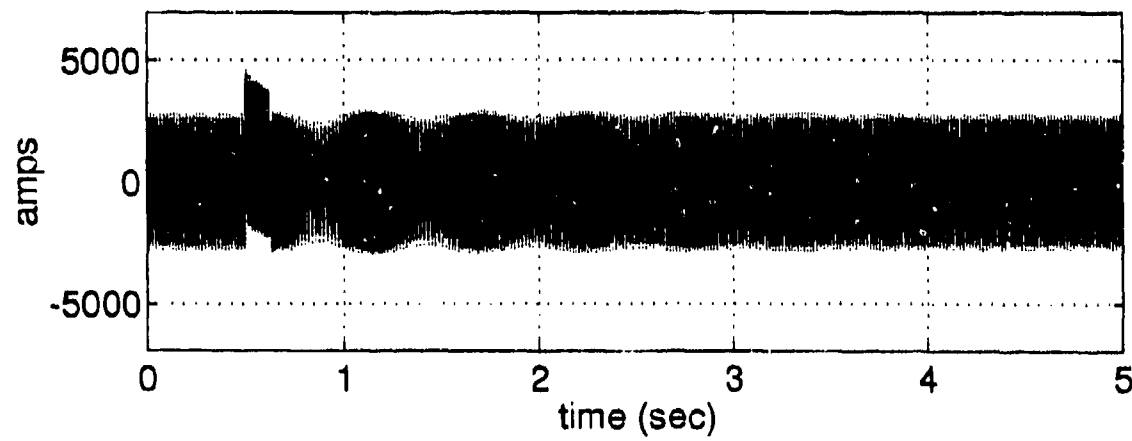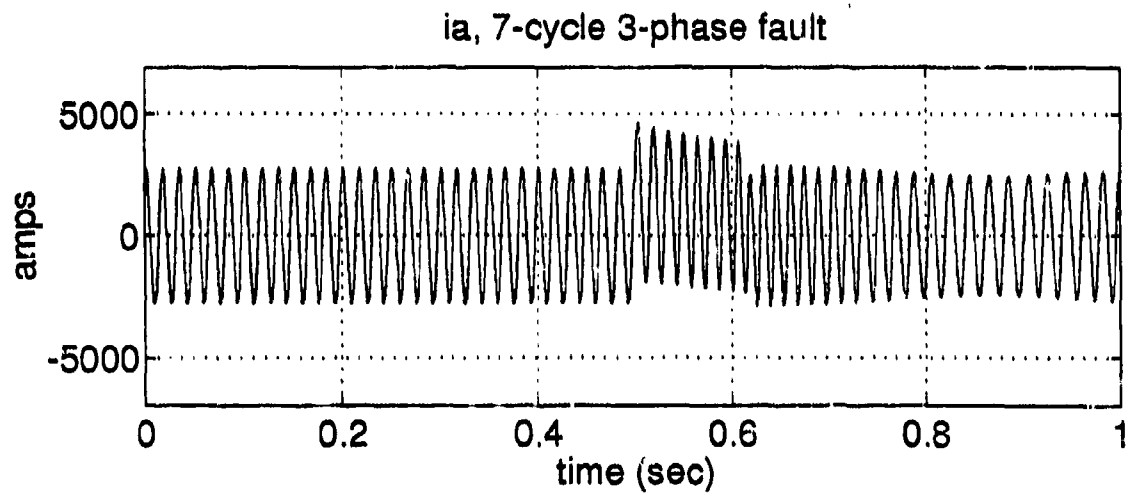
field, 7-cycle 3-phase fault
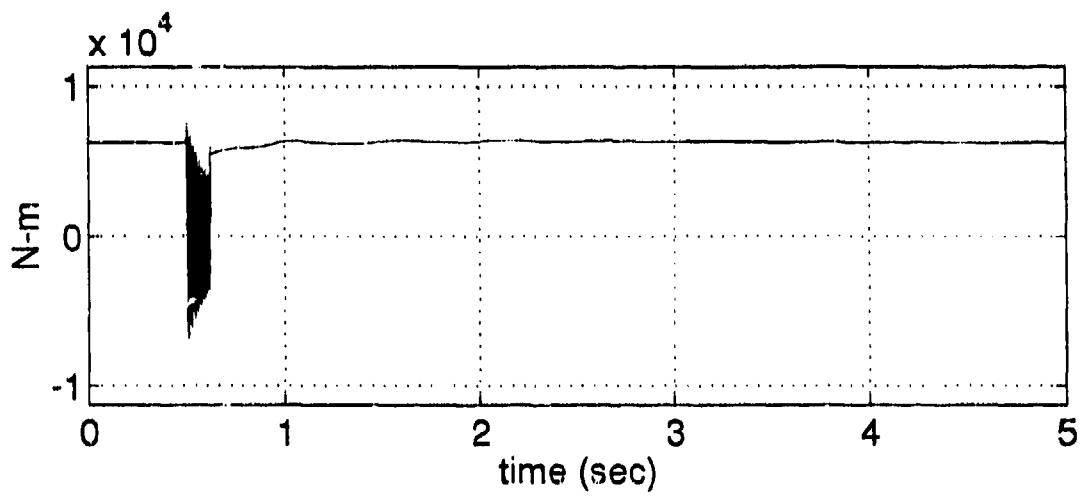
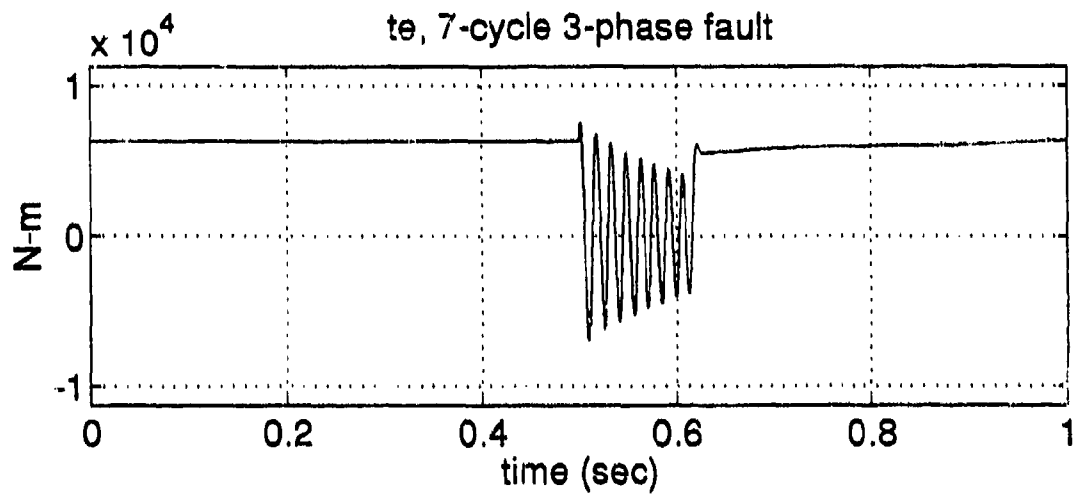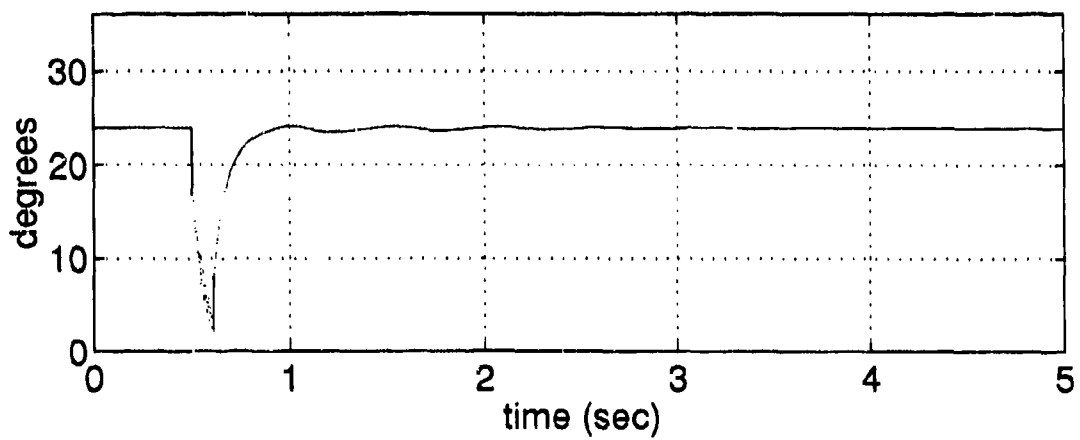Figure 26.  7-Cycle, 3-Phase Fault, *field voltage.*

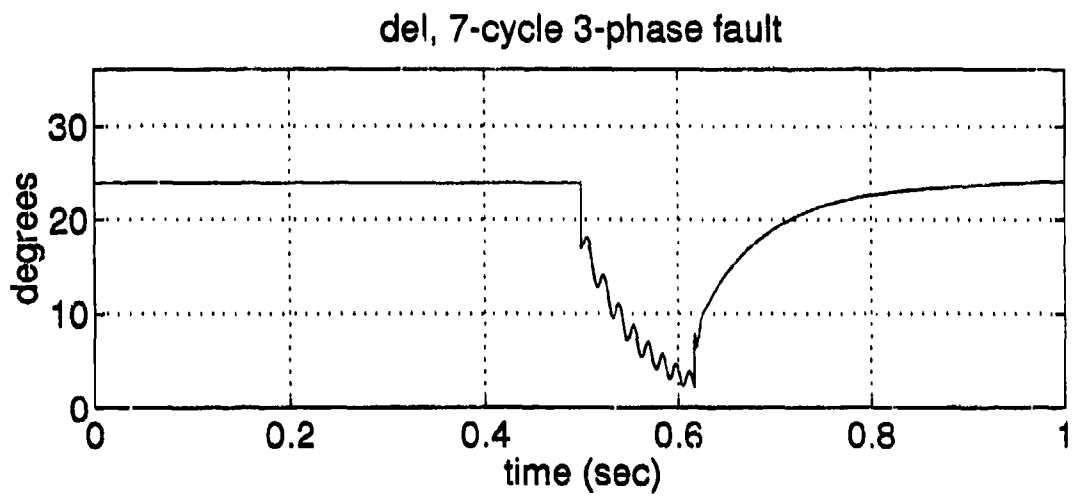Figure 27. 7-Cycle, 3-Phase Fault, *ia*.

57

Figure 28. 7-Cycle, 3-Phase Fault, *te*.

del, 7-cycle 3-phase fault

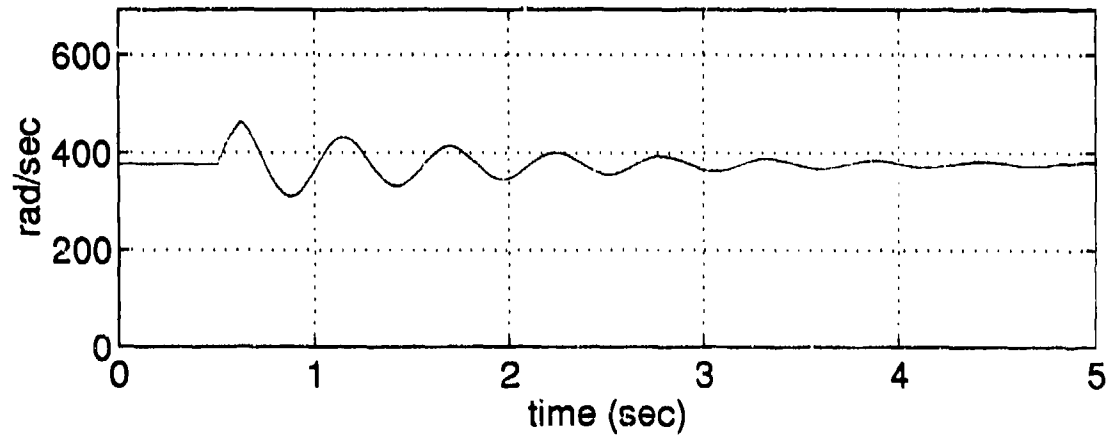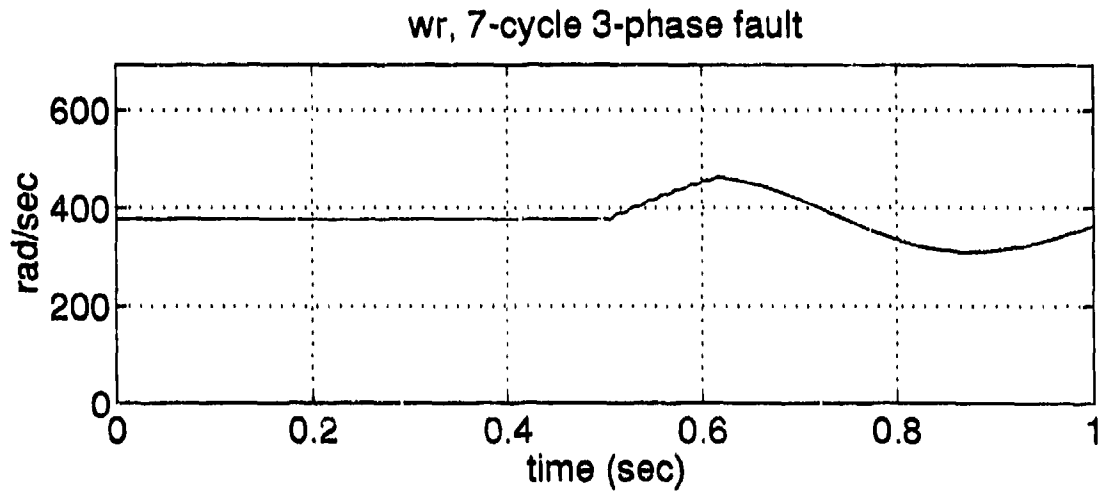Figure 29. 7-Cycle, 3-Phase Fault, *rotor angle (del)*.

59

Figure 30. 7-Cycle, 3-Phase Fault, *rotor speed* ($\omega_r$).

# V. CONCLUSIONS

## A. ADVANTAGES

The advantages to studying naval power system components in a graphical environment are many. To be able to see, in real time, any line or load parameter (i.e. current or voltage) makes the study of system component interaction very straightforward.

The concept of "closing the loop" to make the input and output of the machine dependent on one another, as opposed to the infinite bus concept, is easily implemented with the graphical tools available. Navy power systems definitely require this non-infinite bus modeling due to their capacity difference as compared with commercial power grids.

## B. ANALYSIS OF SIMULINK

Matlab's SIMULINK is an excellent tool for the type of studies conducted in this thesis. Model building and integration into the "power system" was easily done.

One of the difficulties with SIMULINK included the algebraic loop problem necessitating an integrator in the path to provide a time delay element. In this particular study this was not a problem due to the resulting differential equations, however, a possible purely resistive load would be troublesome.

On the issue of speed of the simulations, naturally one is always looking for a faster simulation. I began my research on a 486-33MHz machine, then graduated to a SPARC-2 machine and realized a speed difference of about two times. I then moved to a SPARC-10 and achieved a speed increase of approximately four times over the SPARC-2. Typical times to run a simulation of approximately 5-seconds was about 4-hours on the SPARC-10. In comparing this to a non-graphical simulation tool such as Advanced Continuous Simulation Language (ACSL) [9], a comparable model runs approximately in real time (60

61

seconds of run time data in approximately 60 seconds). The disadvantage of ACSL is, of course, the inability of the user to observe system output in real time and the non-modular modeling of systems.

## C.    FUTURE WORK

The modeling of additional load components including induction machines, another synchronous generator sharing the load, parallel RL-loading, and adjustable speed drives could all be performed in SIMULINK. As the number of integrators in the complete model increases, however, the run time will also increase. In addition, the existing RL-load can be examined under such conditions as critical clearing time, first swing transient stability limit, and various fault conditions such as single line to ground faults, line-to-line faults, etc.

In addition, voltage regulator stability can be studied to find gain limits for this particular regulator. Different regulator designs could also be examined.

Mathworks has also advertised a software package which will take existing SIMULINK models and compile them; this will supposedly increase simulation speed considerably. This product sounds very encouraging.

# LIST OF REFERENCES

[1]     Park, R.H. "Two-Reaction Theory of Synchronous Machines-Generalized Method of Analysis-Part I," *AIEE Trans.*, Vol. 48, July 1929, pp. 716-727.

[2]     Krause, Paul C., *Analysis of Electric Machinery*, McGraw-Hill, Inc., 1987.

[3]     *SIMULINK Dynamic System Simulation Software*, The MathWorks, Inc., Natick, Mass., February 1993

[4]     Krause, Paul C. and Wasynczuk, O., "Development of Computer Models to Analyze Shipboard Electrical Power Systems," Final Report, Contract No. N61533-89-D-0037, School of Electrical Engineering, Purdue University, West Lafayette, IN, October 1990

[5]     *MATLAB, High-Performance Numeric Computation and Visualization Software*, The Mathworks, Inc., Natick, MA., February 1993

[6]     Arrillaga, J., Arnold, C.P., *Computer Analysis of Power Systems*, John Wiley & Sons Ltd., 1990.

[7]     Krause, P.C., Final Report on "Modeling of Shipboard Electric Power Distribution System," for David Taylor Research Center, SBIR Phase I Contract No. N00167-88-C-0031, P.C. Krause and Associates, Inc., West Lafayette, IN, July 1988

[8]     Mayer, C.B., "Digital Computer Simulation Program for Turbine Emulator Drive and Load System," Report of Contract N00167-85-C-0131. May 13, 1987.

[9]     *Advance Continuous Simulation Language (ACSL)*, Mitchell and Gauthier Associates (MGA) Inc., Concord MA., 1993

# BIBLIOGRAPHY

Anderson P.M. and Fouad A.A., *Power System Control and Stability*, Iowa State University Press, 1977.

Glover J.D. and Sarma M., *Power System Analysis and Design*, PWS-Kent Publishing Company, 1989.

Sarma, M., *Synchronous Machines, Their Theory, Stability, and Excitation Systems*, Gordon and Breach Science, 1979.

Stevenson, W.D., *Elements of Power System Analysis*, McGraw-Hill, Inc., 1982

# INITIAL DISTRIBUTION LIST

1.  Defense Technical Information Center                                     2
    Cameron Station
    Alexandria, Virginia    22304-6145

2.  Library, Code 52                                                          2
    Naval Postgraduate School
    Monterey, California    93943-5002

3.  Chairman, Code EC                                                         1
    Department of Electrical and Computer Engineering
    Naval Postgraduate School
    Monterey, California    93943-5121

4.  Professor Robert W. Ashton, Code EC/Ah                                    1
    Department of Electrical and Computer Engineering
    Naval Postgraduate School
    Monterey, California    93943-5121

5.  Professor Harold A. Titus, Code EC/Ts                                     1
    Department of Electrical and Computer Engineering
    Naval Postgraduate School
    Monterey, California    93943 5121

6.  Professor Stephen Williams                                               1
    Department of Engineering
    Baylor University
    PO Box 97356
    Waco, Texas 79798-7356

7.  LT Daniel Kline                                                           2
    3708 Yates Ave. No.
    Crystal, Minnesota   55422

8.  Jack Stowe                                                               1
    6670 Vernon Ave. S.  #110
    Edina, Minnesota   55436